NAVAL POSTGRADUATE SCHOOL

MONTEREY, CALIFORNIA

THESIS

TRACK SCORE PROCESSING OF MULTIPLE DISSIMILAR SENSORS

by

Dimitrios Patsikas

June 2007

Thesis Co-Advisors:	Phillip E. Pace Murali Tummala Gamani Karunasiri
Second Reader:	James B. Michael

Approved for public release; distribution is unlimited

THIS PAGE INTENTIONALLY LEFT BLANK

REPORT DOCUMENTATION PAGE	*Form Approved OMB No. 0704-0188*

1. AGENCY USE ONLY *(Leave blank)*	**2. REPORT DATE** June 2007	**3. REPORT TYPE AND DATES COVERED** Master's Thesis

4. TITLE AND SUBTITLE Track Score Processing of Multiple Dissimilar Sensors

5. FUNDING NUMBERS

6. AUTHOR(S) Dimitrios Patsikas

7. PERFORMING ORGANIZATION NAME(S) AND ADDRESS(ES)
Center for Joint Services Electronic Warfare
Naval Postgraduate School
Monterey, CA 93943-5000

8.PERFORMING ORGANIZATION REPORT UMBERS

9. SPONSORING /MONITORING AGENCY NAME(S) AND ADDRESS(ES)
U. S. Missile Defense Agency

10.SPONSORING/MONITORING AGENCY REPORT NUMBER

11. SUPPLEMENTARY NOTES The views expressed in this thesis are those of the author and do not reflect the official policy or position of the Department of Defense or the U.S. Government.

12a. DISTRIBUTION / AVAILABILITY STATEMENT	**12b. DISTRIBUTION CODE**
Approved for public release; distribution is unlimited	A

13. ABSTRACT (maximum 200 words)

In this thesis, a data fusion problem when a number of different types of sensors are deployed in the vicinity of a ballistic missile launch is studied. An objective of this thesis is to calculate a scoring function for each sensor track, and the track file with the best (optimum) track score can then be used for guiding an interceptor to the threat within the boost phase. Seven active ground-based radars, two space-based passive infrared sensors and two active light detection and ranging (LIDAR) sensors are used to track the ballistic missile in the boost phase. Each space-based platform carries one passive infrared sensor and one LIDAR. For the threat scenario, an IMPULSE intercontinental ballistic missile model is used to create the trajectory of a generic ballistic threat. The IMPULSE model is developed by the National Air and Space Intelligence Center to provide an accurate representation of ballistic missiles. Each sensor provides a track of the missile in the boost phase by using a multiple hypotheses tracking algorithm with an extended Kalman filter. The calculation of the track scoring function is to identify the sensor with the best track file. A track score is calculated for each sensor based on the kinematics of the missile flight parameters and the signal-to-noise ratio at the sensor. By using likelihood ratios, the optimum track file of the threat can then be determined and the corresponding track file can be transmitted to the battle manager control in order to lead the interceptor vehicle against the threat using the track file with the best score. Using the optimum track file scoring signal processing techniques developed in this thesis, the best track file can be sent to the interceptor to destroy the ballistic threat. This leads to a faster response management where the threat can be destroyed inside the territory of the country which launched the threat before any countermeasures are deployed.

14. SUBJECT TERMS Ballistic missiles, Defense networks, IR and LIDAR sensors, Space-borne sensors, Data fusion, Likelihood ratios	**15. NUMBER OF PAGES** 79
	16. PRICE CODE

17. SECURITY CLASSIFICATION OF REPORT	**17. SECURITY CLASSIFICATION OF THIS PAGE**	**19. SECURITY CLASSIFICATION OF ABSTRACT**	**20. LIMITATION OF ABSTRACT**
Unclassified	Unclassified	Unclassified	UL

NSN 7540-01-280-5500
100Standard Form 298 (Rev. 2-89)

Prescribed by ANSI Std. 239-18

THIS PAGE INTENTIONALLY LEFT BLANK

Approved for public release; distribution is unlimited

TRACK SCORE PROCESSING OF MULTIPLE DISSIMILAR SENSORS

Dimitrios Patsikas
Lieutenant, Hellenic Navy
Bachelor of Science, Hellenic Navy Academy, 1996

Submitted in partial fulfillment of the
requirements for the degree of

MASTER OF SCIENCE IN APPLIED PHYSICS
and
MASTER OF SCIENCE IN ELECTRICAL ENGINEERING

from the

NAVAL POSTGRADUATE SCHOOL
June 2007

Author: Dimitrios Patsikas

Approved by: Phillip E. Pace
Co-Advisor

Murali Tummala
Co-Advisor

Gamani Karunasiri
Co-Advisor

James B. Michael
Second Reader

Jeffrey B. Knorr
Chairman, Department of Electrical and Computer Engineering

James H. Luscombe
Chairman, Department of Applied Physics

THIS PAGE INTENTIONALLY LEFT BLANK

ABSTRACT

In this thesis, a data fusion problem when a number of different types of sensors are deployed in the vicinity of a ballistic missile launch is studied. An objective of this thesis is to calculate a scoring function for each sensor track, and the track file with the best (optimum) track score can then be used for guiding an interceptor to the threat within the boost phase. Seven active ground-based radars, two space-based passive infrared sensors and two active light detection and ranging (LIDAR) sensors are used to track the ballistic missile in the boost phase. Each space-based platform carries one passive infrared sensor and one LIDAR. For the threat scenario, an IMPULSE intercontinental ballistic missile model is used to create the trajectory of a generic ballistic threat. The IMPULSE model is developed by the National Air and Space Intelligence Center to provide an accurate representation of ballistic missiles. Each sensor provides a track of the missile in the boost phase by using a multiple hypotheses tracking algorithm with an extended Kalman filter. The calculation of the track scoring function is to identify the sensor with the best track file. A track score is calculated for each sensor based on the kinematics of the missile flight parameters and the signal-to-noise ratio at the sensor. By using likelihood ratios, the optimum track file of the threat can then be determined and the corresponding track file can be transmitted to the battle manager control in order to lead the interceptor vehicle against the threat using the track file with the best score. Using the optimum track file scoring signal processing techniques developed in this thesis, the best track file can be sent to the interceptor to destroy the ballistic threat. This leads to a faster response management where the threat can be destroyed inside the territory of the country which launched the threat before any countermeasures are deployed.

THIS PAGE INTENTIONALLY LEFT BLANK

TABLE OF CONTENTS

THIS PAGE INTENTIONALLY LEFT BLANK

LIST OF FIGURES

THIS PAGE INTENTIONALLY LEFT BLANK

LIST OF TABLES

THIS PAGE INTENTIONALLY LEFT BLANK

ACKNOWLEDGMENTS

First of all I would like to thank my wife Theodora for her support and patience during my studies in Naval Postgraduate School.

Also I would like to thank Hellenic Navy which provided my studies in the United States.

I would like to thank my advisors Prof. Phillip E. Pace, Prof. Murali Tummala, and Prof. Gamani Karunasiri for their important contribution during the research work and their valuable directions according to the theoretical parts of this thesis.

Finally I want to thank The United States Missile Defense Agency for their continued support.

THIS PAGE INTENTIONALLY LEFT BLANK

EXECUTIVE SUMMARY

During the past twenty years — specifically after the first war in the Persian Gulf where ballistic missiles were used for first time after World War II — the global community started to realize the danger of ballistic missiles. An example is the case where these weapons are controlled by terrorist groups or imperialistic governments. Western governments, having realized the magnitude of the problem, started to develop programs with different types of sensors placed on different platforms in order to create a shield against the ballistic missile threat for their territories and their allies.

The main problem for the deployment of all these sensors under the control of a central battle manager control is the evaluation of the sensor's results and the subsequent analysis. The battle manager control needs to know in only a few seconds the exact position of the threat missile and its profile in order to send the appropriate interceptor. The goal is the destruction of the missile within the boost-phase of the missile flight.

The geographical area of the scenario chosen for this thesis' engineering analysis and program development is chosen without any political motivation. Also the type of the threat missile that is used in the study is an unclassified experimental model that is generic.

For the threat scenario, an IMPULSE intercontinental ballistic missile (ICBM) is used to generate an attack against a distant country. The IMPULSE model is developed by the National Air and Space Intelligence Center to provide an accurate trajectory of ballistic missiles.

In this thesis seven active ground based radars are deployed in the vicinity of a ICBM launch site in order to monitor its activity. Also, two low earth orbit (LEO) satellites containing passive infrared sensors (IR) and active light detection and ranging (LIDAR) sensors are deployed in order to monitor the ballistic launch site. The first three active ground based radar sensors (RF#1, RF#2 and RF#3 in Figure 1) are placed close enough to each other so as to evaluate the performance of the likelihood ratio theory

developed in this thesis with regard to the track scoring issues. The other four active ground based radar sensors (RF#4 to RF#7) are placed at different random positions as depicted in Figure 1.

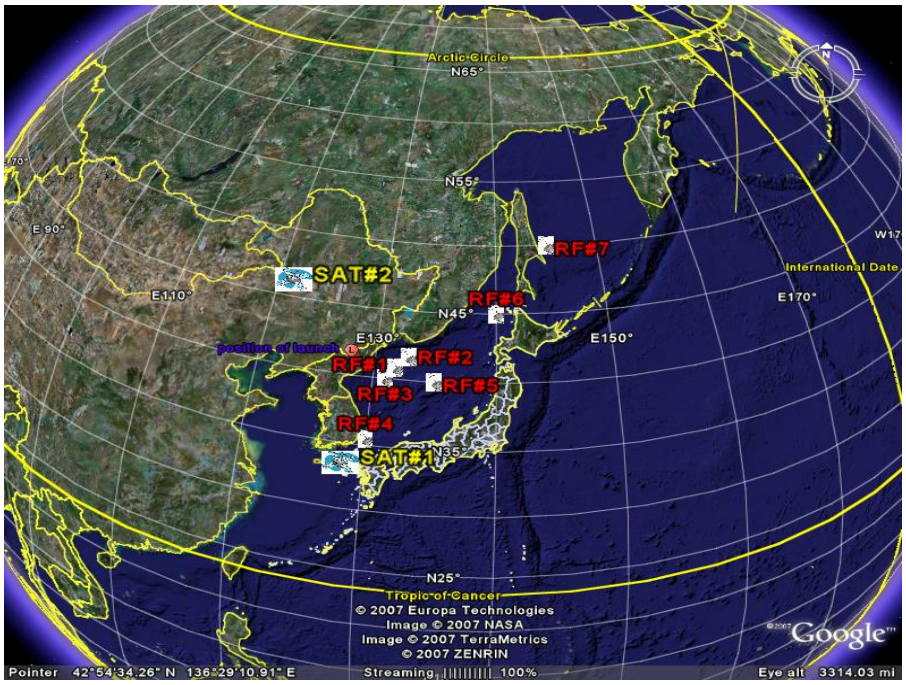

Figure 1. Geographical area of the scenario (From:2007 Google/2007 NASA/2007 Europa Technologies Image)

For each active and passive sensors located along the missile trajectory, the signal-to-noise ratio (SNR) is developed as a figure of merit to measure their ability to track the threat during its boost phase trajectory. The two IR sensors and two LIDAR sensors are placed as shown in Figure 1. On both satellites (**SAT#1** and **SAT#2)** there is one passive IR sensor and one LIDAR. Figure 2 depicts the SNR for the first infrared sensor on **SAT#1** as a function of time. The green line represents the upper stage, which the missile follows after the separation of the booster. The red line represents the lower stage of the booster.

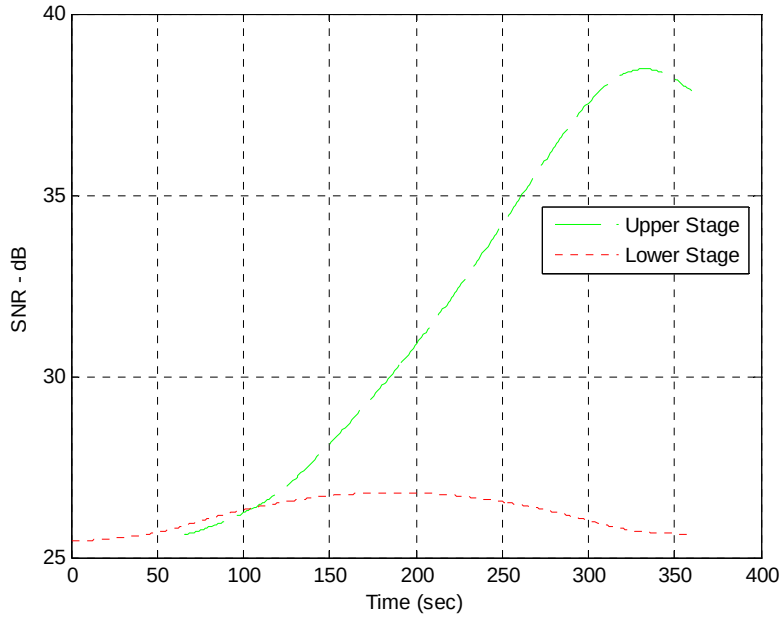

Figure 2. SNR versus Time for the First IR sensor on SAT#1.

The use of passive infrared sensors placed on LEO satellites is very important as this provides the capability of early warning of the launch of a ballistic missile based on its radiation during the first few seconds of the flight as well as the discrimination of the warhead from other objects, which separate themselves from the body of the missile during the flight. Such objects are the booster and debris. The drawback of IR sensors is that they provide only angular information about the target. For this reason, an active laser sensor is placed on the same platform with the IR sensor in order to provide to the IR system the third dimension of range, enabling the ability to perform 3D data fusion.

The calculation of the track scoring function is to identify the sensor with the best track file. A track score is calculated for each sensor based on the kinematics of the missile flight parameters and the SNR at the sensor. By using likelihood ratios, the optimum track file of the threat can be determined and the corresponding track file can be transmitted to the battle manager control in order to lead the interceptor vehicle against the threat. Using the optimum track file scoring techniques developed in this thesis, the best track file can be sent to the interceptor to guide it to the ballistic threat. This leads to a faster response management where the threat can be destroyed inside the territory of the

country that launched the missile before the missile employs any countermeasures. Figure 3 shows the track score for three RF sensors as a function of time (or scans) and demonstrates that during the threat engagement, some sensors have a higher track score at certain times while others have a higher track scores at other positions of the threat flight. The objective of the track score processing is to calculate the track score for each track and select the optimum track that should be used to drive the interceptor.

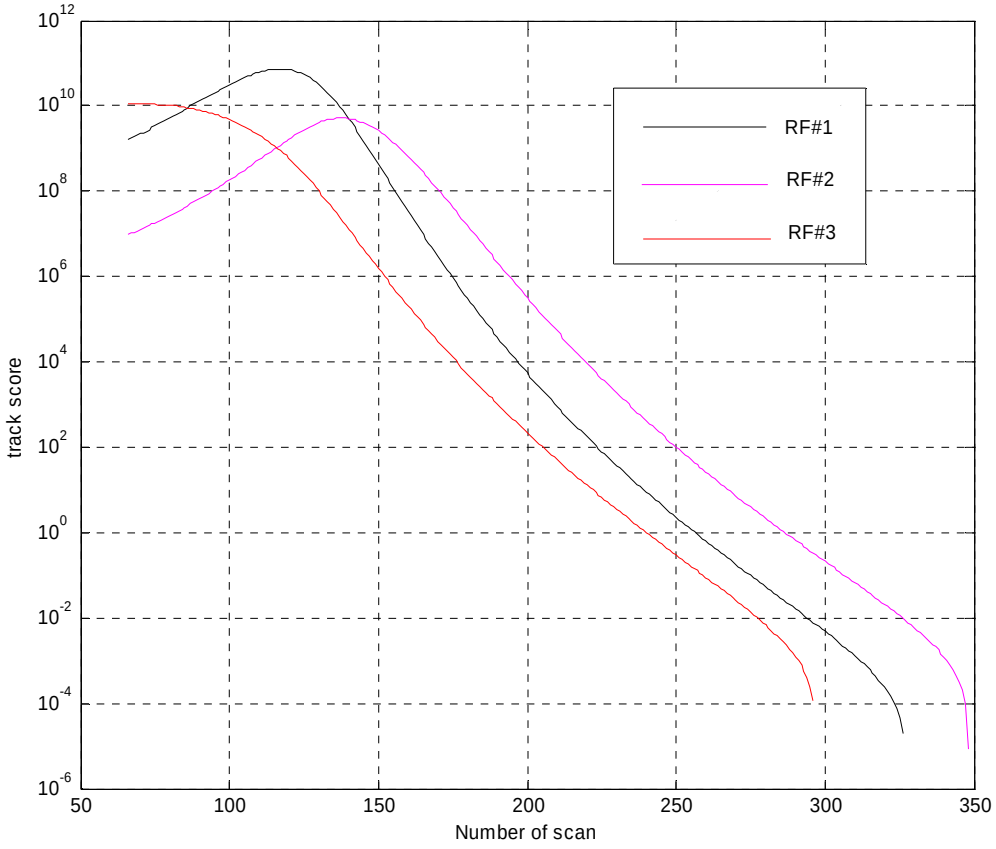

Figure 3. Track score for the first three active sensors

Based on the result of the data fusion, it is inferred that at the beginning of the flight the third radar (RF#3), which is closer to the threat at the beginning, has the best track score. As the flight time continues, the first radar (RF#1) then provides the best track score for the next fifty seconds. Finally, the second radar (RF#2) dominates, presenting the best track score until the end of the boost phase.

I. INTRODUCTION

Over a decade ago, after the fall of the Soviet Union, when the world strived to understand why there was so much hatred among the nations, Henry Kissinger made these comments:

"The end of the Cold War has made such a strategy largely irrelevant. Barely plausible when there was only one strategic opponent, the theory makes no sense in a multipolar world of proliferating nuclear powers. Mutual destruction is not likely to work against religious fanatics; desperate leaders may blackmail with nuclear weapons; blackmail or accidents could run out of control. And when these dangers materialize, the refusal to have made timely provisions will shake confidence in all institutions of government. At a minimum, the rudiments of a defense system capable of rapid expansion should be put into place." [1].

With this, the experience of these years in our minds, the picture of the world right now is exactly depicted by these comments. Local conflicts among the nations have arisen in order to attain goals, which had been hidden for many years under the pressure of a bipolar control system of two super powers.

A TRACK SCORE PROCESSING OF MULTIPLE DISSIMILAR SENSORS

Ballistic missiles are one of the diplomatic tools used by countries to exert pressure on others, and fortunately, until now, their use has been restricted. What happens if this situation does not remain under control? At this moment, several countries around the world have the capability to build such missiles and exert their supremacy. Moreover, many of them have the capability of incorporating mass destruction warheads into these weapons, making the situation a grave concern, not only critical for the opponent's rival, but also for all the other nations due to the possibility of a nuclear threat or accident.

Against that threat, the most technologically-advanced, wealthy nations are developing advanced missile capabilities and, in parallel, are working on systems that provide the capability to defend their nation and their allies. The creation of an early warning network of different types of sensors is the goal in this regard in order to cover

all possibilities of attack from every edge of the earth. Specifically, these networks will include radars, infrared (IR) sensors and light detection and ranging sensors (LIDAR) which will be placed on terrestrial, airborne or spaceborne platforms.

The ballistic missile's flight can be divided into three phases: boost, midcourse and terminal. The boost phase extends over the first four minutes (approximately) of the missile's flight and varies according to whether or not the fuel that is used is either liquid or solid. The main goal of these sensors is to form a surveillance network to detect and track a ballistic missile threat from the launch and throughout the boost phase. The interception of the missile during the boost phase provides several significant advantages for the defender. The destruction of the missile during the boost phase provides a greater chance that debris and remains of the missile will fall into the territory of the country that launched the missile. Second, the missiles do not have the chance to deploy countermeasures against an interceptor. Finally, if the effort during the boost stage is not successful there is time to defeat the threat in the next stages. This thesis work is focused entirely on the boost phase of the threat.

B. PREVIOUS WORK AND OBJECTIVE

This thesis is a continuation of the work started by Rakdham [2] who examined a scenario involving the launch of ballistic missiles against the United States from North Korea, developed the multiple hypothesis tracking and extended the theory of the linear assignment problem (LAP). The LAP theory was initially developed by Danchick and Newman [3] to provide an alternate approach to solving the related data association problem by minimizing computational requirements. Rakdham [2] also used the IMPLUSE model from NASIC in his work.

The main goal of this thesis is to examine the issue of track scoring for the different dissimilar sensors within the surveillance network and the data fusion process of the raw data being delivered over the surveillance network. Data fusion is then the selection and the compromise of the accumulated data, which will be transferred to the battle manager control (BMC), turning the raw data being collected into decision level knowledge for the interceptor guidance.

C. PRINCIPAL CONTRIBUTION

The major tools employed in this effort include the IMPULSE simulation tool for launch of the ballistic threats and the MATLAB simulation software. The IMPULSE simulation tool was developed by the National Air Space Intelligence Center (NASIC) and provides the trajectory for a given ballistic missile, which is necessary for the creation of the required data files. These data files are then processed by the MATLAB code developed in [2], which (a) modeled each of the RF sensors, (b) performed the multiple hypothesis tracking and (c) developed the linear assignment problem and solution. This thesis extends the effort in [2] by including additional IR and LIDAR sensor systems within the surveillance architecture and also increasing the number of RF sensors that are used.

The IMPULSE program was used as a tool for analyzing the trajectory file of ballistic missiles. This program has the capability to provide all aspects of the kinematics during the flight of the missile, such as the position, the velocity, the acceleration, the change of the mass and the change of the drag force on the missile. Also it provides the capability of virtually viewing the flight as a function of time.

Next, the radar cross section (RCS) of the ballistic missile was examined in order to deploy a more dynamic aspect of the radar equation, which would be necessary in the tracking function and data fusion process. The calculation of the RCS is based on the geometry of the trajectory and the incident angle of the beam on the missile.

After this step, more sensors are added in the vicinity of the launch site in order to evaluate their response against the ballistic threat missile. Two infrared (IR) and two LIDAR sensors are placed on two spaceborne platforms (low orbit satellites). That is, every spaceborne platform contains one IR and one LIDAR sensor. The satellites are deployed close to the vicinity of the launched missile to provide good coverage. Finally, having the responses of each sensor within the surveillance network, the track scoring and data fusion signal processing could be developed.

D. THESIS OUTLINE

Chapter II introduces the sensors for the data fusion system developed in this thesis and also discusses their implementation in the MATLAB code. It begins with a definition of the SNR of the IR sensors and analyzes all the parameters that must be taken into account. It also develops the IR sensor model, which will be placed on the low-earth orbit (LEO) satellite. The second section of this chapter analyzes the LIDAR sensor SNR. At the beginning, the SNR formula of the LIDAR sensors is developed by covering all the necessary aspects. After the definition of the SNR, the LIDAR model of the simulation is introduced. The chapter ends by providing the parameters of the deployed radars and the evaluation of the missile's RCS.

Chapter III discusses the data fusion of the tracks of deployed sensors. The theory of likelihood ratio is developed based on the contribution of the kinematics and the sensor signals.

Chapter IV depicts the scenario considered. Specifically it provides the positions of the sensors and their responses to the ballistic missile. Also, the result of the data fusion problem for the radar sensors is presented.

Chapter V presents a summary and the concluding remarks.

Finally, Appendix presents the flow chart of the MATLAB code used in the simulation.

II. SENSOR DESIGN

This chapter presents two space based sensors (infrared and light detection and ranging system) and one radio frenquency sensor (radar). The signal to noise ratio and design considerations of these sensors are discussed in depth.

A. IR SENSOR

The signal-to-noise ratio (SNR) is the figure of merit used in this work in order to evaluate the track quality of an infrared sensor. Also, it is known that the SNR is the basic figure of merit for all the sensors with respect to the design and evaluation of their ability to perform target tracking and detection. In order to define the SNR of a system, it is necessary to determine the ratio of the signal power to the noise power.

1. SNR of an IR Sensor

First, SNR is defined for the best case in which the background is not taken under consideration, assuming a blue sky background. The signal power which a sensor can calculate from a point source is given by:

$$H = \frac{J}{R^2} \quad \text{W cm}^{-2} \tag{2.1}$$

where J is the radiation intensity in Wsr^{-1} and R is the range to the target in centimeters.

Note that (2.1) does not consider any atmospheric absorption. Including the transmission losses due to atmospheric absorptions in the (2.1) yields:

$$H = \tau(R)\frac{J}{R^2} \quad \text{W cm}^{-2} \tag{2.2}$$

The effect of transmission loss in an IR system is a very important consideration in determining the performance of such a system. There are three major parameters that characterize atmospheric attenuation [4]: space extinction, emission, and turbulence.

The transmittance is a measure of the atmospheric attenuation of the energy from a light source or target and is given by [3]

$$\tau(R) = 1 - e^{-\beta R} \tag{2.3}$$

where R is the range, and β is the sum of the two attenuation parameters: absorption β_a, and scattering β_s. The transmittance though the atmosphere is presented in Figure 4.

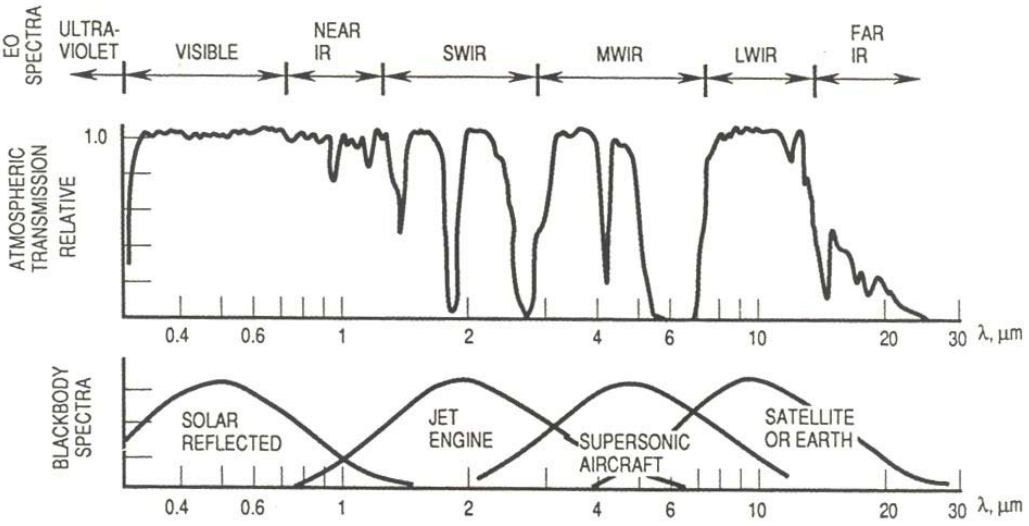

Figure 4. Atmospheric absorption and scattering (From: 10)

As shown in Figure 4, there are three IR bands available for applications: short-wave IR (SWIR), which is in the 1-2.7 μm wavelength, the midwave IR (MWIR), which is in the 3-5 μm wavelength, and the longwave IR (LWIR), which is in the 8-14 μm wavelength. For each one of these bands, the parameter β is very complicated to determine with respect to all the atmospheric characteristics, such as rain, fog, clouds, haze, and so on. Standard computer models for obtaining parameter β are available [4],[5].

The amount of energy that an IR sensor can receive from a source depends on the aperture of its lens. Given that the aperture is d (m), the amount of energy that the sensor receives is called the *irradiance* and is given by:

$$S = \tau(R)\frac{J}{R^2}\frac{\pi d^2}{4} \quad [\text{W}] \tag{2.4}$$

As with all sensor systems, such as radar, the energy measured by the system at the antenna is not the final energy the system uses to calculate target position. This is because there are many sources of noise inside the system. In fact, in an IR system, there are two types of noise: the background noise, which it is not considered initially for the calculation of the SNR, and the noise in the sensor.

The noise in the sensor can be categorized as Johnson noise, shot noise, generation-recombination noise, temperature noise, microphonic noise, 1/f noise, and finally electronic-interface noise [6].

Then the internally generated noise power, called noise equivalent power (NEP), is given by [6]:

$$NEP = 1/D \tag{2.5}$$

where D is the Detectivity of the sensor. Note that this detectivity can also be a function of wavelength $D(\lambda)$.

Finally, the specific Detectivity, D^*, another figure of merit for IR systems is defined as [3]:

$$D^* = \frac{(A_d \Delta f)^{1/2}}{NEP} \tag{2.6}$$

where Δf is the equivalent noise bandwidth, and A_d is the effective sensor area.

All of the system losses, such as losses due to optics, electronics and detector, are accumulated in a loss factor L, which is applied to (2.4) and results in the signal power at the detector as

$$S = \tau(R) \frac{J}{R^2} \frac{\pi d^2}{4} L \text{ [W]} \tag{2.7}$$

In the following analysis, the sensor is considered to be operating in a staring model. The advantage of this model is that all of the detectors are considered to cover the field of view (FOV) for the entire time frame [6]. In this case, the number of pixels is equal to the number of detectors in the array, so the time frame (τ_f) to scan the entire

image is equal to the dwell time (τ_d), the time required to read all of the pixels, which is expressed by

$$\tau_f = \tau_d . \tag{2.8}$$

As a result, the equivalent noise bandwidth Δf, which is also the signal bandwidth [6] page 489, is equal to:

$$\Delta f = \frac{1}{2\tau_f} = \frac{1}{2\tau_d} \tag{2.9}$$

The instant field of view (IFOV) α_d can be obtained from the detector area and the focal number $(f/\#)d$ and is given by:

$$\alpha_d = \frac{A_d}{\left[(f/\#)d\right]^2} \tag{2.10}$$

where A_d is the detector area. Finally, combining (2.6) to (2.10) allows us to express the SNR as

$$\frac{S}{N} = \frac{\pi d JD^* L}{4(f/\#)R^2}\left(\frac{\eta\tau_f}{\Omega}\right)^{1/2} \tag{2.11}$$

where Ω is the solid angle, which the FPA observes, in steradians.

2. Space-borne IR Sensor Design

The simulation developed in this thesis employs two IR spaceborne sensors, located at different positions around the Earth, both in the vicinity of the launched missile. The satellites are in a low-earth, sun-synchronous orbit (LEO) at an altitude of 705 km, crossing the equator at the same local time on each pass. Their ground velocity is 6.76 km/sec; therefore, it takes approximately 90 min for a single revolution around the Earth and requires 16 days to revisit the same location on the Earth's surface. Note that the satellites are assumed to be stationary for this simulation. Otherwise, the simulation

has to take into account the relative motion between the spaceborne platforms and the ballistic missile, which makes the problem more complicated and is beyond the scope of this work. The modeling parameters used for the two IR spaceborne sensor satellites are taken from the Landsat 7 satellite [7]. This is National Aeronautics and Space Administration's (NASA) most recent model and is used for commercial reasons, assuming that a rotating telescope with 1000×1000 detectors in the focal plane array for better resolution of the target, which means better discrimination of multi targets at the same area. Another assumption is that only band number 6 (out of eight bands) in SWIR is used. The Landsat 7 parameters are summarized in the Table 1 [7].

Parameters	Units
Ground resolution	185 m
Wavelength	2-2.35 μm (SWIR)
Spectral bandwidth	10 nm
IFOV	262.4 μ radians
Telescope diameter	55mm (2in)
Optical f/#	6
Number of detector per spectral band	1000×1000
Detectivity	3.5×10^{10} cm-Hz$^{1/2}$/W
Loss factor	0.085

Table 1. Sensors Parameters

The basic source of the infrared energy from a ballistic missile is the hot exhaust plume. The other sources of infrared energy are the exhaust nozzle of the engine and the aerodynamic heating of the missile [8]. This work does not consider the latter two parameters, only focusing on the radiation from missile's plume. An estimate of the

magnitude of this radiation intensity can be made by taking into account the size and the temperature of the associated plume observed by the detector [8].

Right after the launch, the size of the plume is 4 m in diameter and about 50 m long, and the temperature of the plume at the nozzle is about 1800 K. Using an average temperature of 1400 K, the highest radiance exitance can be calculated from the blackbody equation and is 7×104 Wm^{-2}-μm^{-1} at a wavelength λ of 2.1 μm. Assuming that the plume is a blackbody and radiates isotropically, then the resultant radiation intensity is approximately 3 MW/sr. As the target rises, it comes closer to the sensor and results in an increase in the radiation intensity due to an expansion in the size of what the detector can observe as well as the associated decrease in the atmospheric absorption. For the purposes of this simulation, the radiation intensity is assumed to be a constant at its peak value of 3 MW/sr.

As mentioned in the beginning of the section, the detector is a rotating telescope that uses the focal plain array (FPA) technology. The detector is a cooled mercury cadmium telluride (HgCdTe). FPA technology is very important for the discrimination of ballistic missile at the boost face, using more color bands [9]. Specifically, two bands are used, one before and one after the burnout. The HgCdTe provides a detection capability across many wavelengths from the SWIR to very long wavelength (14 μm).

The detectivity of the IR sensors used in this simulation is estimated from Figure 5 for a wavelength of 2.1 μm. The values of detectivity in this figure were derived from an analysis of commercial detectors, under background- limited conditions, at the temperature of 300 K and an IFOV of 180^{o} [10]. In this case, it is also assumed that a filtered, cooled detector at a temperature of T = 77 K was used. Taking into account all these assumptions, the detectivity from Figure 5 is equal to 1.5×10^{10} cm-$Hz^{1/2}$/W.

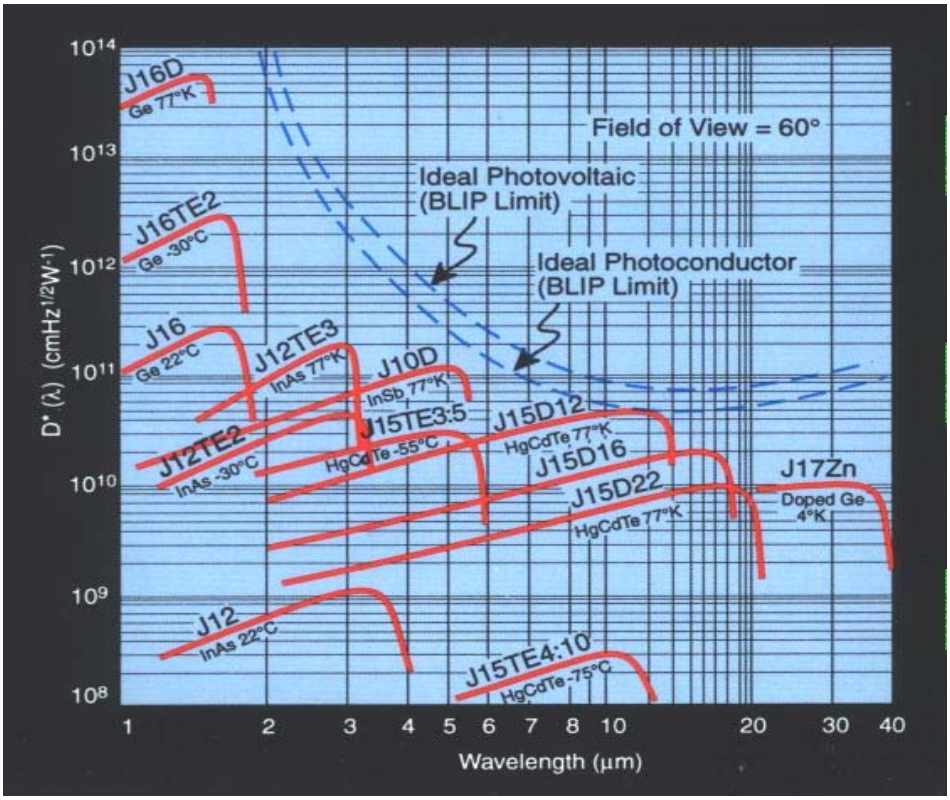

Figure 5. D* for commercial detectors (From: [10])

At this point, the energy from the terrain, called background IR, is analyzed. The analysis covers only the first four minutes of the missiles' trajectories in the boost-face. During this interval, the background energy comes only from the terrain as the missile has not reached the peak of its altitude; therefore, the satellite looks only at the terrain. Otherwise, as the missile rises into the space, the background will change making the problem more complicated.

At the wavelengths of 2 to 2.35 μm, the background energy from the terrain is generated by the reflection of the solar radiation [11]. This energy is calculated assuming that the terrain is a blackbody source at a temperature of T = 300 K. For wavelengths between 3-5 μm, the background energy is considered negligible due to the atmospheric absorption [11]. It takes large values of background energy for wavelength above the 5 μm, which does not affect this work. Figure 6 depicts the energy from the background.

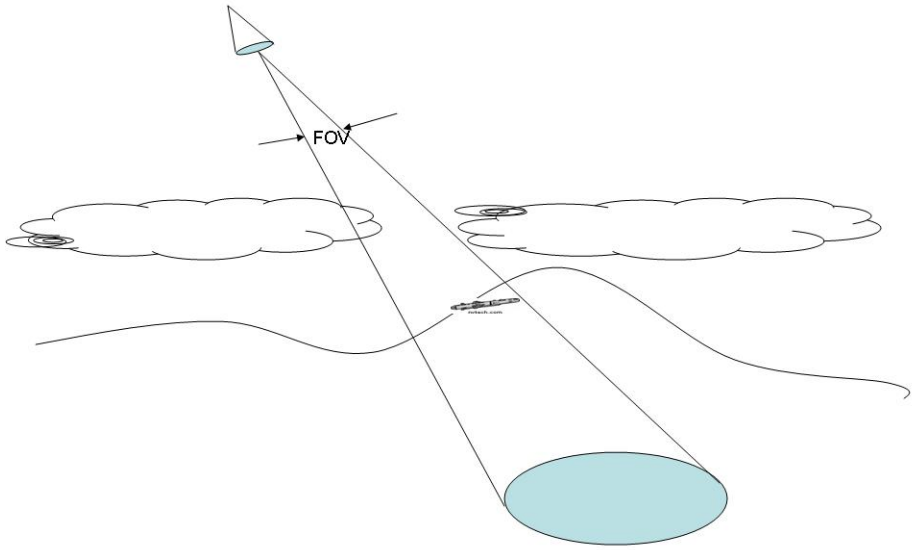

Figure 6. IR signal from the missile and the background (After: [11])

The background energy from the terrain at a wavelength of 2.1 μm is calculated as:

$$M(\lambda) = 2\frac{\pi hc^2}{\lambda^2} \cdot \frac{1}{e^{\frac{hc}{kT}} - 1} = 5220 \quad \text{W/cm}^2\text{-}\mu\text{m} \tag{2.12}$$

As a matter of fact, this is not the background energy, which the detector measures because the detector is cooled. Figure 7 depicts the geometry of a cold detector.

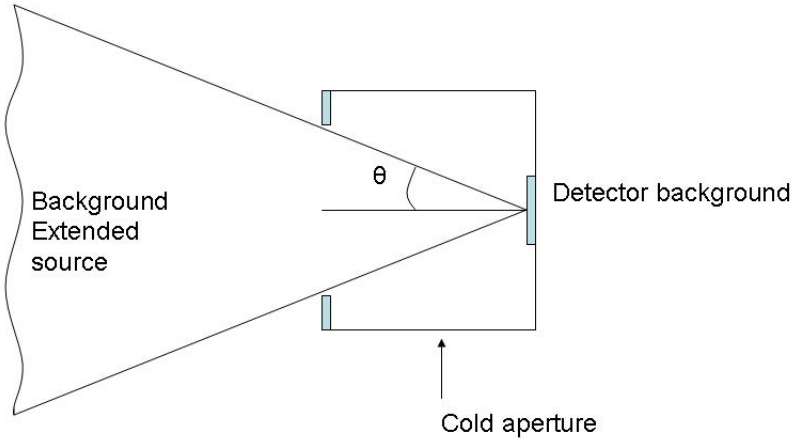

Figure 7. Cold detector geometry (From:[8])

The detector background is then given by

$$E_{background} = \pi M(\lambda)\Omega = 30.33 \text{ dB} \tag{2.13}$$

The total solid angle coverage is computed by the elevation coverage angle and the azimuth coverage. The elevation coverage angle:

$$\in = \arctan\left(\frac{185}{705}\right) = 14.7^{o} \tag{2.14}$$

The azimuth coverage angle is given by:

$$h = \arctan\left(\frac{185}{705}\right) = 14.7^{o} \tag{2.15}$$

Finally, the total solid angle :

$$\Omega = \frac{\in \cdot h}{57.3^2} = 0.0658 \text{ sr} \tag{2.16}$$

The scan geometry of the employed spaceborne sensors is shown in Figure 8.

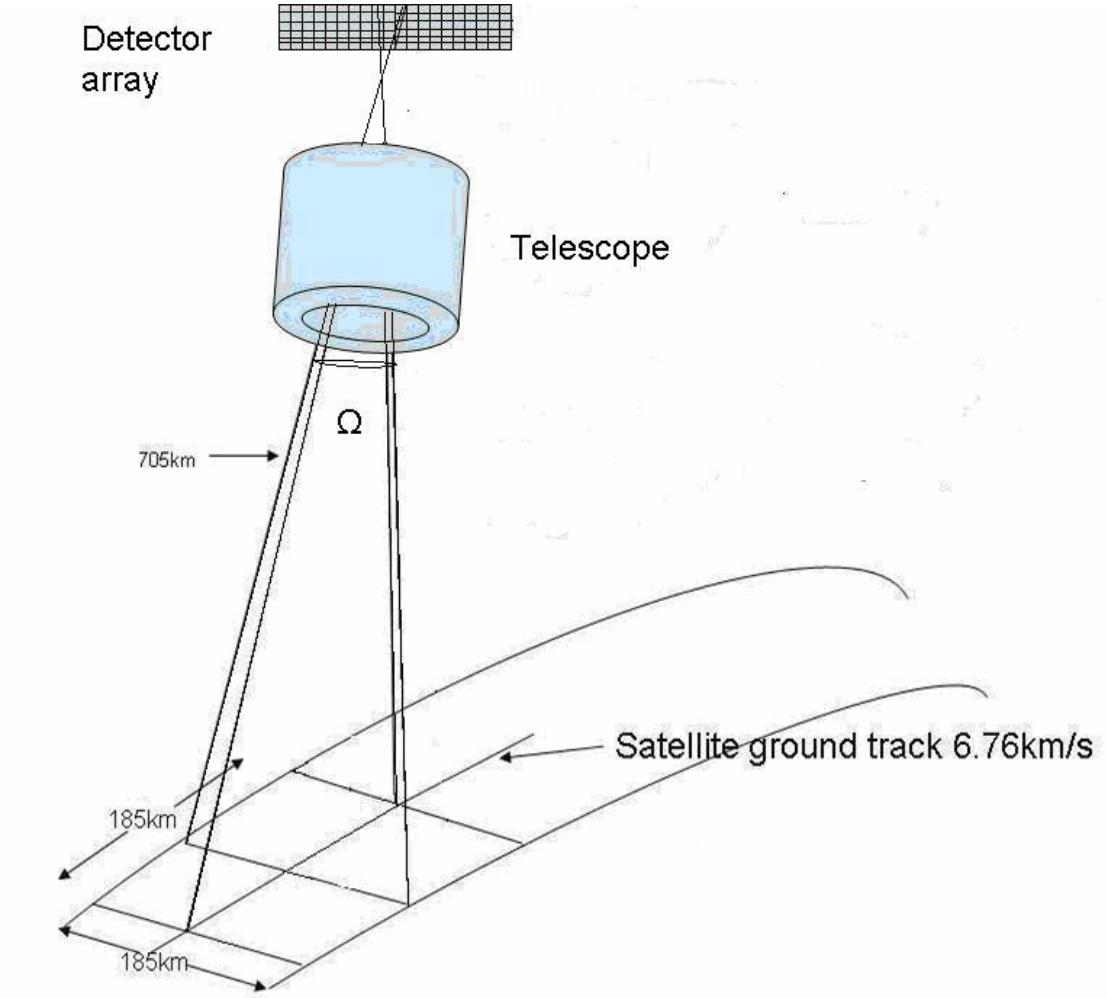

Figure 8. Scan geometry (After: [10])

The number of the resolution cells (pixels) is calculated as:

$$P = \frac{\Omega}{a_d^{1/2}} = \frac{0.0658}{\left(262.4 \cdot 10^{-6}\right)^{1/2}} \sim 1 \text{ Mpixels} \tag{2.17}$$

Figure 9 depicts the SNR value of the IR sensor #1 placed at the satellite platform SAT#1 by using (2.11) for SNR in MATLAB. In order to calculate the SNR, it is assumed that the range of the missile is provided to the IR sensor by the laser sensor as described in the following section. The simulation calculates the SNR for a 3D geometry instead of a 2D geometry.

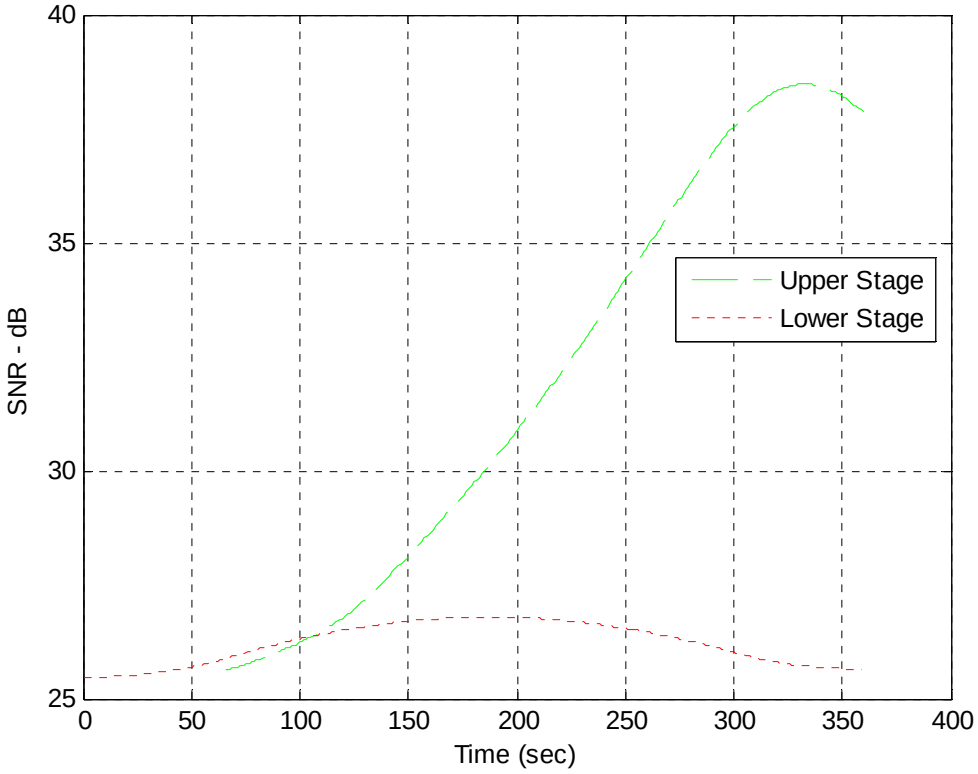

Figure 9. SNR versus time for a IR system at the platform SAT#1

From Figure 9, the SNR is about 25 dB at the beginning of the flight and is a reasonable value for detecting a ballistic missile. Also, it can be mentioned that after the separation from the booster at time $t = 65\,\text{sec}$, the missile rises closer to the sensor having a peak SNR value of 38 dB.

B. LIGHT DETECTION AND RANGING SYSTEM

This section presents a derivation of the SNR of the light detection and ranging systems (LIDAR). Also, spaceborne LIDAR design issues are briefly discussed.

1. SNR of a LIDAR Sensor

LIDAR systems are similar to radar systems. They are active systems as they illuminate the target in order to achieve the parameters of the target position. Compared to a conventional radar, the beamwidth of a LIDAR is very small due to its operation at

very high frequencies. This trait gives them the capability of high resolution. On the other hand, due to the narrow beamwidth, they have limited search capability. For this reason, they are used in conjunction with other electro-optical systems. An example of these systems is the laser range finder (LRF) which is used together with a forward looking infra-red (FLIR). LRF provides the range, in addition to the angular data from the FLIR, to a Kalman filter to form a 3D track.

In the design of a LIDAR system, the atmospheric absorption has to be taken into account. As shown in Figure 2, the electromagnetic radiation through the atmosphere at μm wavelengths specifies two bands where the laser radar can be applied. These windows are at the 1.06 μm and 10.6 μm wavelengths. At 1.06 μm, the system uses neodymium YAG crystal lasers, and at the 10.6 μm the system uses CO_2 gas lasers.

The following derivation for the SNR is taken from [10]. To define the SNR, it is necessary to calculate the signal power received by a LIDAR detector. The distribution of signal power over a spherical area is given by:

$$P = \frac{P_t}{4\pi R^2} \tag{2.18}$$

where P_t is the transmitted power and R is the distance of the target.

The focusing effect of the lens in order to direct the transmitted power in a specified direction is given by:

$$L = \frac{4\pi}{\frac{\pi}{4}\theta_{BW}^2} \tag{2.19}$$

where θ_{BW}^2 is the beamwidth.

In this case, it is assumed that the ballistic missile is a Lambertian target, so the power reflected by the target is distributed over a hemispherical area. For this reason, the signal power is divided by the factor $1/\pi R^2$.

Finally the signal power is given by:

$$S = \frac{PA\tau_o\rho}{2\pi R^2} \tag{2.20}$$

where ρ is the target backscattering coefficient, τ_0 is the optical efficiency and A is the lens aperture area.

The above form covers the case in which the laser beam is much smaller than the target area. Otherwise, we should take the target cross section σ into account. Then the signal power takes the form:

$$S = \frac{2PA\sigma\tau_o\rho}{\pi^2 R^4 \theta_{BW}^2} \tag{2.21}$$

where θ_{BW} is the parameters of lens. By substituting $\theta_{BW} = \lambda / D$, where λ is the wavelength and D is the lens diameter, (2.21) takes the form:

$$S = \frac{8PA^2\sigma\tau_o\rho}{\pi^3 R^4 \lambda^2} \tag{2.22}$$

From [10], the detector noise level is determined. The LIDAR detectors are of two types. The direct (or nonconherent) sensors, which accumulate the energy in a way similar to the electro-optic sensor, and the coherent (heterodyne) sensor in which a phase difference between the transmitted and the received signals is utilized. In this case, the range is measured by the Doppler phenomenon. In this simulation, coherent sensors are used.

The NEP for a LIDAR is given by the form:

$$NEP = (A_d \Delta f)^{1/2} / D^* \tag{2.23}$$

where D^* is the detectivity, Δf is the receiver bandwidth , and A_d is the detector area .

Finally, by taking into account (2.16) and the noise level for a heterodyne receiver as given by [10], NEP is obtained as:

$$NEP = (hf / j)(B) \tag{2.24}$$

where j is the quantum efficiency, B is the receiver bandwidth, h the Planck's constant and f is frequency .

The SNR of the LIDAR system is then given by:

$$SNR = \frac{S}{NEP} = \frac{8PA\rho\tau_o\sigma}{\pi^3 R^4 (hf / j)(B)} \tag{2.25}$$

As mentioned at the beginning of Chapter II, this value will be the figure of merit in order to evaluate each track of the spaceborne sensors.

2. Spaceborne LIDAR Sensor Design

This section discusses the design of spaceborne laser sensors. An NdYAD laser system, operating at a wavelength of 1.06μm, is placed on a LEO satellite at an altitude of 705 km around the Earth (along with an IR sensor). The parameters of a typical sensor of this type are listed in Table 2 [10, chapter 8].

Parameters	Units
Detector area	6.25×10^{-4} cm^2
Optics diameter	20 cm
Wavelength	1.06 μm
Pulse power	2 MW
Pulsewidth	10 ns
Target reflectivity	0.1
Detectivity D*	10^{10} cm-Hz$^{1/2}$/W
f /#	2
τ_o: optical efficiency	0.5

Table 2. Parameters of LIDAR system[Ref 10, ch 8]

The inverse of the pulse width defines the receiver bandwidth $B = 1/\tau = 10^6$ Hz. From (2.22), noise equivalent power of the receiver can be written as:

$$\text{NEP} = [(6.25\times10^{-4})(10^6)]^{1/2}/10^{11} = 2.5\times10^{-9}\text{W} \quad (2.26)$$

The range of the missile is calculated by the MATLAB function, LIDARobservation, by using the inputs from the IMPULSE simulation program. In the simulation, it is assumed that the ballistic missile with dimensions of 20 m length and 1.2 m of diameter is a perfect cylinder. As a result, RCS is $\sigma \cong 32$ dBsm.

In Figure 10, the SNR is depicted as a function of time for the LIDAR sensor #1 placed on platform SAT#1 of the simulation.

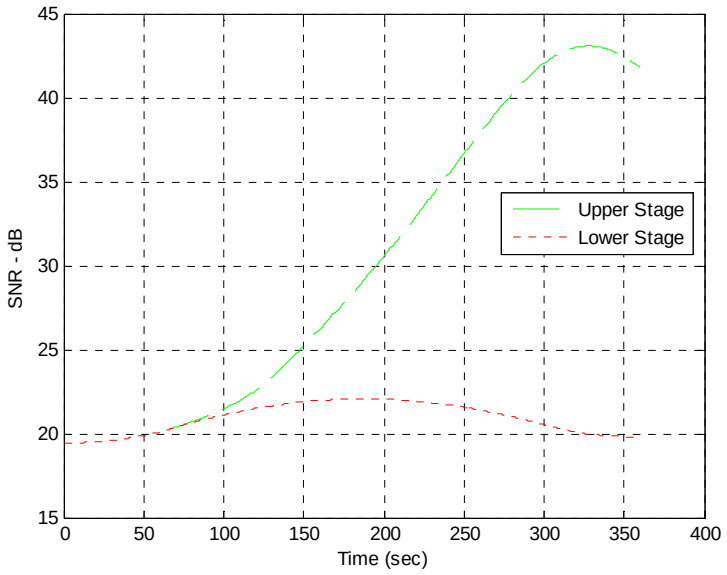

Figure 10. SNR versus time for the LIDAR sensor on SAT #1

C. RADAR DESIGN

Seven radars, which are placed at different locations relative to the launch position, use the same configuration in order to make the analysis easier to verify. In this section the radar model originally developed in [2] and used in the simulation is reviewed

with a summary of the parameters given below in Table 3. The single pulse, signal to noise ratio $(SNR)_1$ for each radar system can be expressed as:

$$(SNR)_1 = \frac{P_t G_t^2 \lambda^2 \sigma}{(4\pi)^3 k T_s B R^4} \tag{2.27}$$

where $T_s = T_a + T_e$, T_e is the receiver noise temperature and T_a is the antenna noise temperature which in the work reported here assumed to be 290 K as was the assumption in [2]. P_t is the peak transmitted power, G_t is the antenna gain, B is the bandwidth of the receiver, σ is the radar cross section of the ballistic threat target, k is Boltzmann's constant. Due to the large unambiguous range required, the pulse repetition frequency (PRF) is modeled as PRF=150Hz.

Table 3 lists the parameters of the radar considered in the simulation.

Parameters	**Values**
Transmitted Power	1 MW
Carrier Frequency	10 GHz
Antenna Gain	42 dB
Radar operating Bandwidth	15 MHZ
Receiver Noise Temperature	290 K

Table 3. Radars parameters [2]

The radar cross section (RCS) of the missile during the flight is calculated by the program POFacets [12]. The missile used in the simulation is a sample unclassified model. To determine RCS of the missile, it is assumed that the missile is a circular cylinder with a radius of 0.60 cm and a length of 20 m.

The angle θ between missile's trajectory vector and the distance vector from the radar to missile, which is required in order to define the RCS function, is determined by the MATLAB function RFobseravation by using the geometry of the Figure 11. From Figure 11, it is inferred that the angle of incidence is computed as the inner product between the vector of distance from the sensor to missile and the vector of the curve. The vector of the curve is defined from the difference of the successive points of the

trajectory. The RCS determination is a 3D problem. In this simulation, it is assumed that the change of the angle takes place only on the x-y axes without taking the third dimension into account.

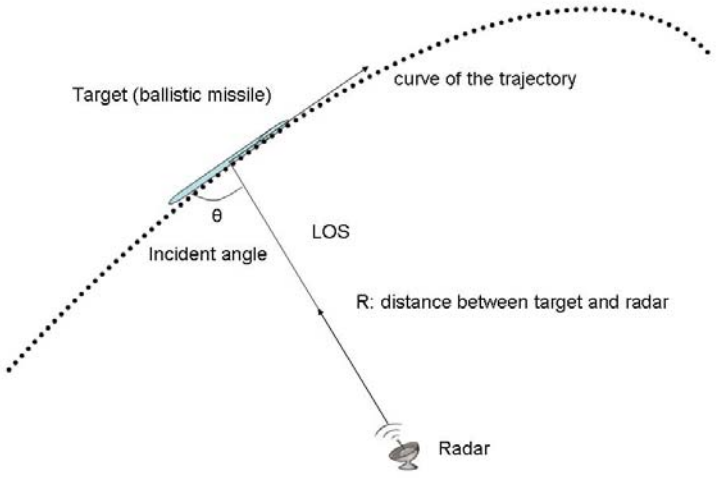

Figure 11. Calculation of incident angle θ

Using the above geometry, the MATLAB function RFobservation calculates the incident angle θ for the first radar sensor and is shown in Figure 12.

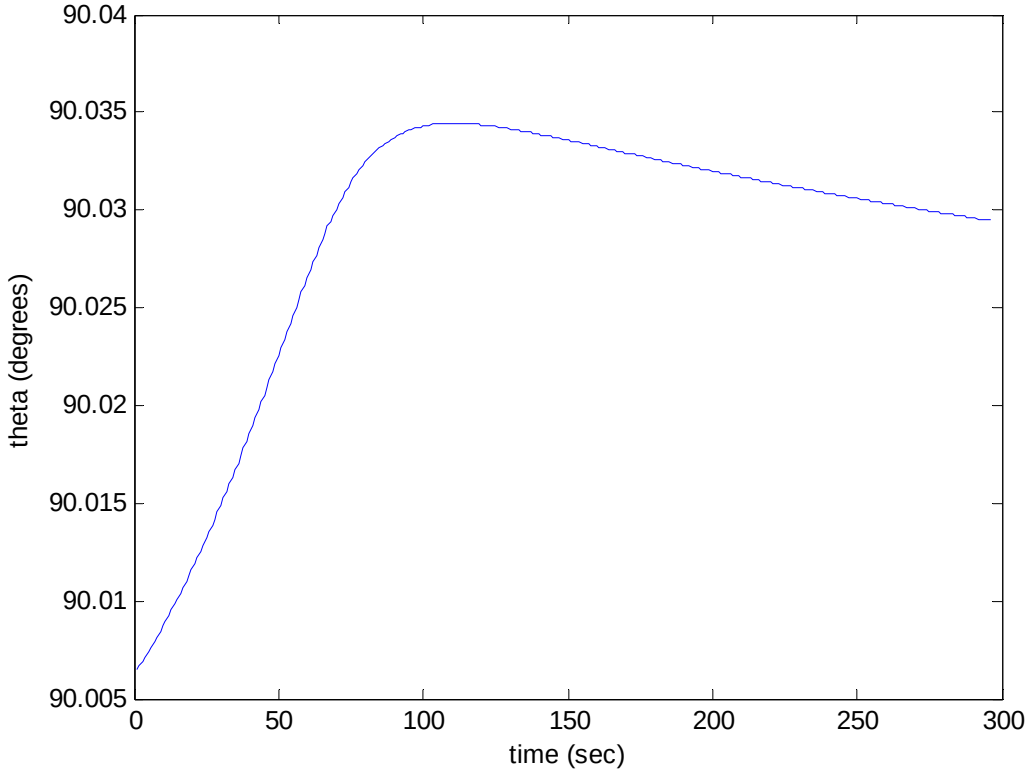

Figure 12. Calculation of incident angle θ

Having determined the incident angle and using the POFacets [12] code, the RCS of the ballistic missile is obtained as shown in Figures 13 and 14.

Figure 13 is a polar plot of the RCS as a function of the angles of incidence. In the vicinity of angle $\theta = 90^0$, which has been calculated from the previous analysis, the values of the RCS are around 36 dBsm.

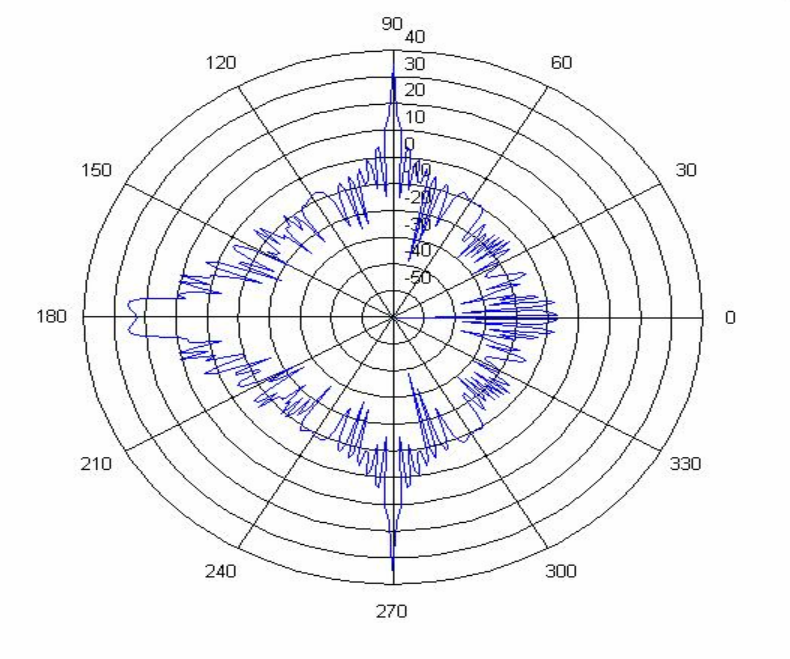

Figure 13. Polar plot of the Ballistic Missile RCS

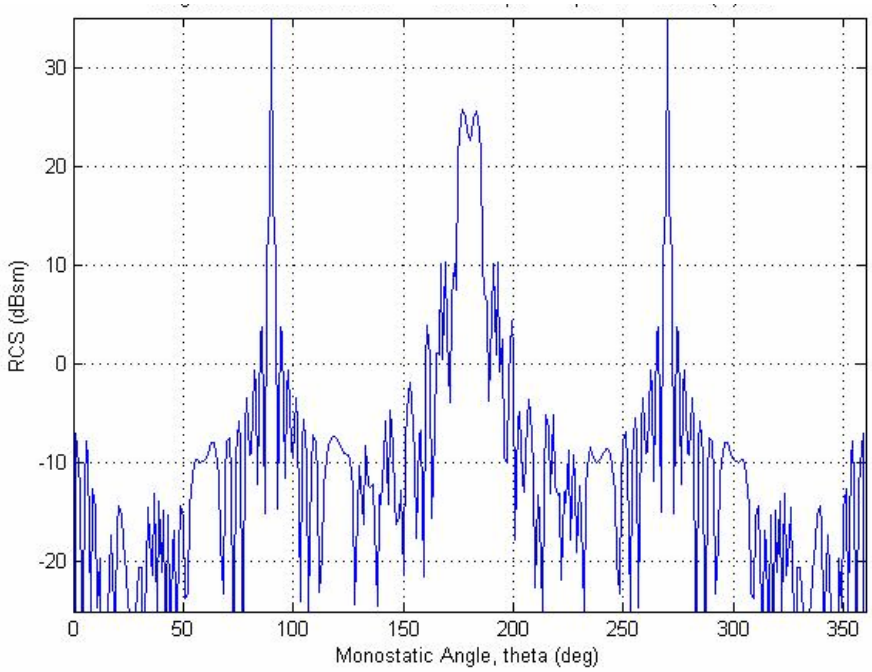

Figure 14. Linear plot of the Ballistic Missile RCS

Figure 14 is a plot of the ballistic missile RCS with respect to the angle of incidence. From the above two plots, it is inferred that the RCS for an angle of incidence in the vicinity of 90^0 is equal to 36 dBsm.

In summary, this chapter described the parameters of the three different types of sensors used in the simulation. The parameters for the IR and LIDAR sensors are listed. Also, the parameters for seven radars at sea level are listed. Next, Chapter III describes the data fusion process and the theory of the likelihood ratios, which is used in the simulation for evaluating the performance of the radars.

III. DATA FUSION PROCESS

Data fusion process is one of the most critical parts of an integrated network of different types of sensors placed on terrestrial, airborne, or spaceborne platforms. The other processes that are part of the data fusion process are the association of the targets, feature extraction and identity declaration. Specifically, data fusion is the procedure of collection, combination and evaluation of information from different sources (sensors), seeking to estimate and predict the level of threat against our friendly positions and units. There are many techniques of collecting and compromising data which depends on the purpose and the design of the system. All these techniques are basically similar as they follow the same philosophy. The difference each time is the place where the association and data fusion take place in an integrated system. In this simulation the series of the procedure is described in Figure 15. [13]

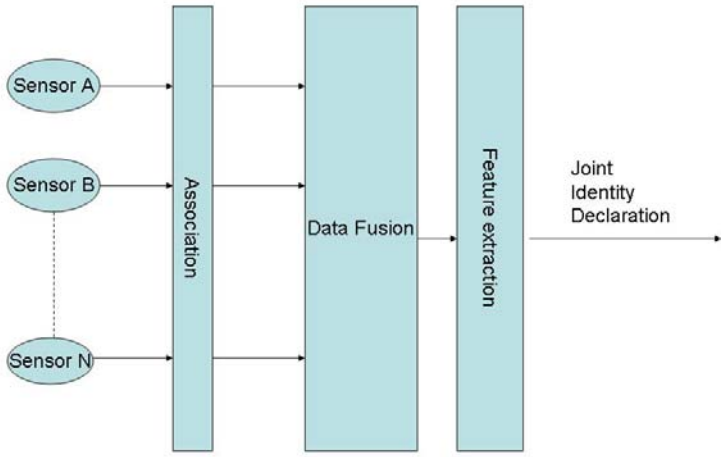

Figure 15. Procedure of identity declaration (From: 13)

From Figure 15, each sensor makes its own association concerning the multiple targets that are present. The association processing of the targets used in this work is according to [2]. Continuing on, the results of the association of each sensor are sent to a fusion center where the data fusion takes place. Then, based on the result of the data

fusion, the feature extraction and finally the declaration of the identity of the target is derived. With other techniques the data fusion comes first in the center and is responsible for the association of the targets as well as the feature extraction and the identity declaration.

There are many advantages to fusion of data from multiple, dissimilar sensors placed in different locations. First of all, the combination of different observations results in an improved estimation of the target's trajectory (velocity, position, acceleration). That means, statistically, using the results of N sensors, the estimated position of the target can be improved by a factor $N^{1/2}$ [14]. Also, by using observations from many sensors, an improved estimated position of the target can be achieved. As an example, consider the triangulation between two sensors that observe the same target [13]. Second, by using different types of sensors, the fusion performance is improved as the information of one sensor can be used to overcome the deficiencies of other types of sensors. For example, the case of an IR sensor alerting a radar to confirm the presence of a target can improve the probability of detection [4, Chapter15]. The IR provides the detection of the target and the angular direction of the target to the radar. Then the radar, by using a longer standard coherent waveform, seeks to confirm the target and attain the range as well as the range rate data. The radar, based on the SNR of the IR system, can lower its threshold in order to adjust the detection performance on the target. As a result, not only an improved detection of the targets takes place, but also the attributes of each sensor are utilized. This is an example of the interpolation techniques, which can take place between different types of sensor (FLIR, LIDAR, airborne sensor, space board systems), in order to cover any aspect of the problem.

Figure 16 depicts the sequence of the procedure of the interpolation techniques described above using a radar and an infrared search and track (IRST) system. In this example, the radar and the IRST use inter-sensor cueing and inter-sensor data sharing to confirm the presence of the target. The data fusion process develops a central tracking file, which is supplied to the sensor management processor. The sensor management process then feeds the processed target results back to the radar and the IRST for refinement.

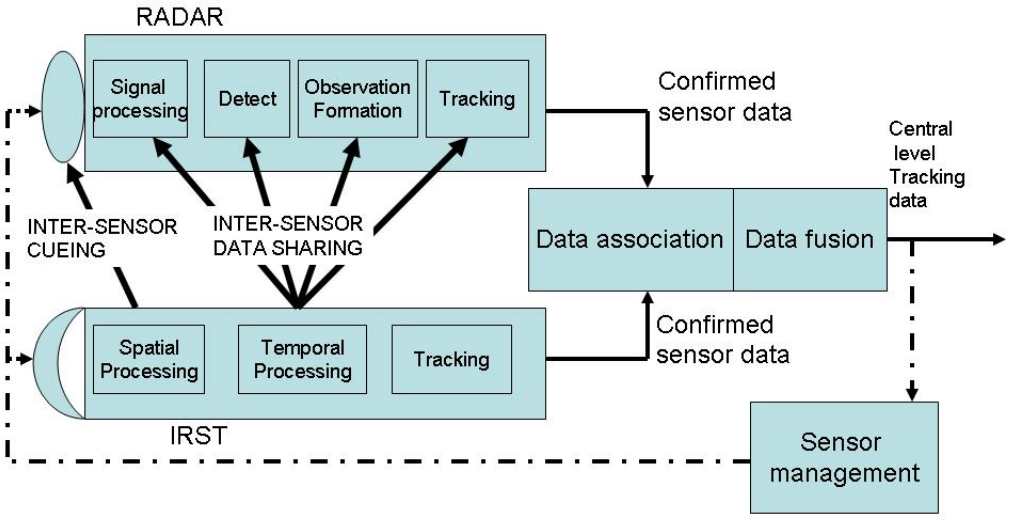

Figure 16. The role of coupled fusion (After: [4])

A. TRACK SCORE FUNCTION

In this section, the likelihood ratio of the kinematic parameters, and the signal parameters, which contribute during the measurement process, are developed. The likelihood ratios are the figure of merit for this work in order to evaluate the track reliability. For this reason, it is called the t*rack score function*.

The likelihood ratio for a combination of data, taking the priori probability data into account, is given by [15, page 73]:

$$\Lambda(H_1, H_0) = \frac{p(D/H_1)Po(H_1)}{p(D/H_o)Po(H_o)} \stackrel{\Delta}{=} \frac{P_T}{P_F} \tag{3.1}$$

where H_1 is the true target hypothesis, H_0 is the false target hypothesis, P_T is the probability of true target, P_F is the probability of false target, $p(D/H_i)$ is the probability density function assuming that the H_i is correct, $Po(H_i)$ is priori probability of H_i.

The performance of the tracking system should be independent of the behavior of the target. The system is evaluated for its ability to respond instantly to any change of the trajectory of the target either in velocity or the direction.

Taking K scans of data, where the measurement error for one is not related to the error from the previous scan, the likelihood ratio (Λ) can be given as the product of the likelihood ratio due to the kinematics (Λ_κ) and the likelihood ratio due to the signal (Λ_s) is given by [4, Chapter 15]:

$$\Lambda(K) = \Lambda o \prod_{K=1}^{K} \Lambda_k \Lambda_s \tag{3.2}$$

where

$$\Lambda o = \frac{Po(H_1)}{Po(H_0)}$$

The initial track score is dependent on the first result of the measurement of the system. As the system starts to count from zero, the kinematics parameters do not play any role in the initial track score. The initial track score can be expressed as [4, Chapter 6]:

$$\Lambda(1) = \frac{Po(H_1)P(Det/H_1)\,p(y_s/Det,H_1)}{Po(H_0)P(Det/H_0)\,p(y_s/Det,H_0)} \tag{3.3}$$

where y_s is the total signal related data (in this work, the signal-related data will be the SNR of the target), $p(y_s/Det,H_1)$ is the probability density function of detection assuming that H_i is correct, $p(y_s/Det,H_0)$ is the probability density function of detection assuming that H_0 is false alarm, and $Po(H_1)$ is the initial probability of target's presence, which, is given by:

$$Po(H_1) = \beta_{NT} V_C \tag{3.4}$$

where V_C is the measurement volume (we assume that every true target detection or false alarm takes part inside of this volume; in this work, V_C is equal to one), β_{NT} is a new target density (assumed equal to unity).

The case of false alarm is given by the $P_0(H_0) = 1$. Additionally, $P_D = P(Det / H_1)$ is the probability of detection and $P_{FA} = P(Det / H_0)$ is the probability of false alarm.

Combining (3.3) and (3.4) and taking $P_0(H_0)$ into account, the initial track score is given by:

$$\Lambda(1) = \frac{\beta_{NT} V_C P_D}{P_{FA}} \frac{p(y_s / Det, H_1)}{p(y_s / Det, H_0)} \tag{3.5}$$

Taking the logarithm of (3.5) yields:

$$\ln \Lambda(1) = \ln[\beta_{NT} V_C] + \ln[\frac{P_D}{P_{FA}}] + \ln[\frac{p(y_s / Det, H_1)}{p(y_s / Det, H_0)}] \tag{3.6}$$

In this work, the initial track score is assumed to be $\Lambda(1) = 0$.

1. Kinematics Related Likelihood Ratio

To determine track score based on the kinematic parameters, it is necessary to introduce gating. Gating is a method of determining which observations are the best to update the tracks. Gating defines cells where the measurements and the observations are included in order to find the best match among them. The scope of gating is to define as small an area as possible, which will include both the measurements and the observation, minimizing the possibility of error. There are many techniques of gating. The cell could have a rectanguloid or an ellipsoid.

The term global nearest neighbor (GNN) is the method used in this work. GNN is the method of association in which each measurement in a track is associated with the nearest neighbor in order to achieve the best update by its closest observation [4, Chapter 1]. Figure 17 depicts the problem of gating.

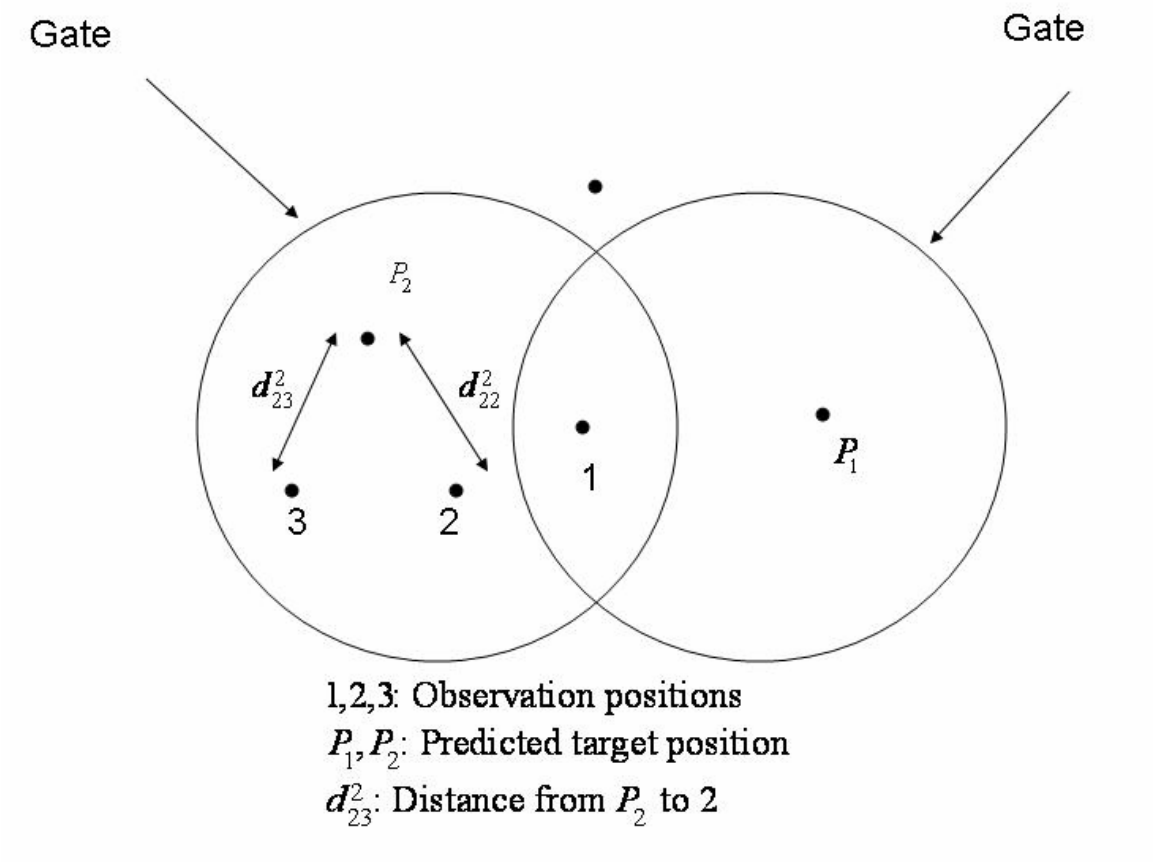

Figure 17. Gating (From[4])

The distance d^2_{22} from predicted target position P_2 to 2, called normalized statistical distance, is given by [4, Chapter 6]:

$$d_{22}{}^2 = \tilde{y}^T S^{-1} \tilde{y} \tag{3.7}$$

where $\tilde{y}$ is innovation (the difference between the actual and expected measurements at every track), S is measurement residual covariance matrix. The innovation $\tilde{y}$ is given by

$$\tilde{y} = y(k) - h(\hat{x}(k/k-1)) \tag{3.8}$$

where h is the nonlinear measurement function for the case of the extended Kalman filter, x is the state vector, $\hat{x}$ is the state estimate vector, $y(k) = h(x(k)) + v(k)$, and v is white Gaussian noise with covariance matrix R and mean zero..

In a nonlinear function like the extended Kalman filter, S^{-1} is given by the following form [4]:

$$S^{-1} = HPH^{-1} + R \tag{3.9}$$

where P is the prediction covariance matrix and H is the measurement matrix.

Taking the gating into account and assuming a Gaussian distribution for the target returns as well as a uniform distribution for the false alarms, the likelihood ratio (Λ_k) for the kinematic part is defined as:

$$\Lambda_k = \frac{V_c e^{(-d^2/2)}}{(2\pi)^{M/2}\sqrt{|S|}} \tag{3.10}$$

where M is the measurement dimension (in this work, it is set to one) and $|S|$ is the determinant of the measurement residual covariance matrix S.

2. Signal Related Likelihood Ratio

Based on likelihood ratio (Λ_s) of the signal-related data, the track score is given by [4, Chapter 6]:

$$\Lambda_s = \frac{P(Det/H_1)\,p(y_s/Det, H_1)}{P(Det/H_0)\,p(y_s/Det, H_0)} \tag{3.11}$$

Taking both P_D and P_{FA} into account, (3.11) can be written as:

$$\Lambda_s = \frac{P_D\,p(y_s/Det, H_1)}{P_{FA}\,p(y_s/Det, H_0)} \tag{3.12}$$

In the case of the radar, when the SNR is available, the signal likelihood ratio is given by (3.11). The Swerling model 3 is typical for the missiles under consideration [4, Chapter 2]. The probability density function under H_i is given by

$$p(y/H_1) = \frac{1+y/(1+2/\bar{\Theta})}{(1+\bar{\Theta}/2)2}\exp[\frac{-y}{1+\bar{\Theta}/2}] \tag{3.13}$$

where y is SNR data and $\bar{\Theta}$ is the average of the SNR.

Probability density function under H_0 is given by:

$$p(y/H_0) = \exp(-y) \tag{3.14}$$

For an IR sensor, the derivation of the probability density function is more complicated. A constant false alarm rate (CFAR) detector is used in order to detect unresolved targets. CFAR detectors are designed to maintain a constant false alarm rate for a specific period of time. For this reason, a CFAR detector normalizes the background clutter by dividing the filter output by sample standard deviation, which is assumed to be known or can be obtained through a Monte Carlo simulation. How this occurs in practice is explained in [15]. Finally, it is known that, by using a sample standard deviation, the SNR follows a t-distribution instead of a Gaussian distribution. That means, the SNR has larger tails and larger values above the threshold. As a consequence, the probability density function under H_1 can be written as

$$P(y/H_1) = \frac{\exp(-\bar{s}^2(1-a^2)/2)}{\sqrt{N\pi}\,2^{(N-1)/2}\Gamma(N/2)(1+y^2/N)^{(N+1)/2}} I(\bar{s},a) \tag{3.15}$$

where

$$a = \sqrt{\frac{y^2/N}{1+y^2/N}}$$

$$I(\bar{s},a) = \int_{-a\bar{s}}^{+\infty} (z+a\bar{s})^N e^{-z^2/2} dz$$

and N is the number of degrees of freedom. For IR systems, N is relatively small. In order to calculate the maximum likelihood value of N, the number of data samples in the tail of the distribution should be calculated first [15]. In this work it is calculated by testing the system performance.

The probability density function under H_0 is given by:

$$P(y/H_0) = \frac{1}{\sqrt{N\pi}} \frac{\Gamma(N+1/2)}{\Gamma(N/2)} \left(\frac{1}{1+y^2/N}\right)^{(N+1)/2} \tag{3.16}$$

In summary, this chapter described the theory of the likelihood ratios used in the simulation. The likelihood ratio formula for the kinematic and the signal-related parameters of the missile is defined in order to calculate the track scoring function for a radar. Next, Chapter IV demonstrates the simulation and the results.

THIS PAGE INTENTIONALLY LEFT BLANK

IV. SIMULATION RESULTS

In this chapter, the simulation of a missile tracking is presented; the IMPULSE model and MATLAB are the tools used to implement the simulation. Specifically, the results from the IMPULSE program are used by the MATLAB code from [2] in order to simulate the tracking problem. The simulation results of the sensor performance based on the likelihood estimation are presented. In this simulation, an unclassified model of the ballistic missile is used. A detailed description of the requirements (inputs) and capabilities (outputs) of the IMPPULSE program are outlined in [2].

Figure 18 depicts the geographical area as well as the positions of the sensors. The geographical area of the scenario chosen is arbitrary. The ballistic missile covers the distance from Asia to North America in approximately at 40 minutes.

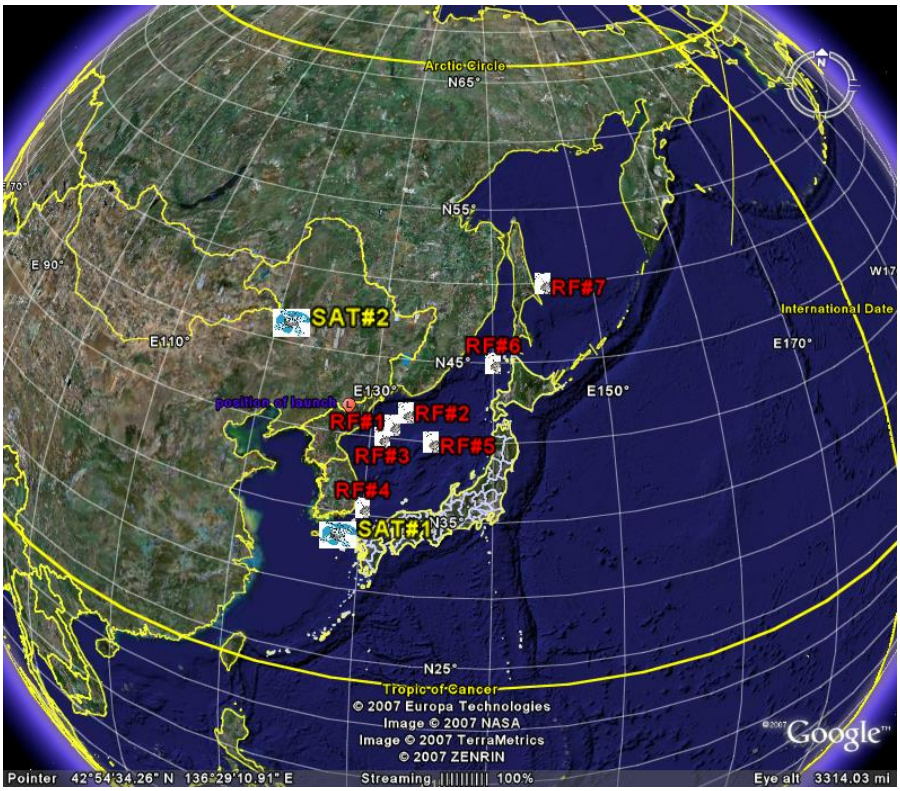

Figure 18. Geographical area of the scenario (From: 2007 Google/2007 NASA/2007 Europa Technologies Image)

In Figure 18, the seven active ground based radars (RF#) and satellites (SAT#) are placed close to the missile launch position. The seven radars have the same parameters (transmitted power, frequency, beamwidth, and PRF) and are at different positions in order to examine the tracking and fusion performance. More radars can be used along the trajectory to cover the entire flight of the missile. The sensor radars used in the simulation are adequate for covering the area depicted in Figure 18.

The IR and LIDAR sensors are placed on the satellite platforms. It is assumed that there are no interactions between them, and the transfer of the data between the two sensors takes place instantly.

Table 4 lists the positions of the sensors in the vicinity of the launched ballistic missile. The radars are placed at the sea level, but the IR and LIDAR are placed at an altitude of 705 km above the sea level.

a/a	Type of sensors	Position		
		Latitude	Longitude	Amplitude
1	RF #1	131°46′44″E	40° 50′45″N	Sea level
2	RF #2	132°46′44″E	41° 40′45″N	Sea level
3	RF #3	131°00′00″E	40° 00′00″N	Sea level
4	RF #4	130°00′00″E	35° 00′00″N	Sea level
5	RF #5	135°00′00″E	40° 00′00″N	Sea level
6	RF #6	140°00′00″E	45° 00′00″N	Sea level
7	RF #7	145°00′00″E	50° 00′00″N	Sea level
8	IR/LIDAR #1	130°00′00″E	35° 30′00″N	705 km
9	IR/LIDAR #2	125°00′00″E	45° 30′00″N	705 km

Table 4. Sensor positions

Figure 19 depicts the same geography of the scenario as in Figure 18 but from a different angle of view. In this depiction, the altitude of the satellites and their place relative to the launch position, L, is clearly presented.

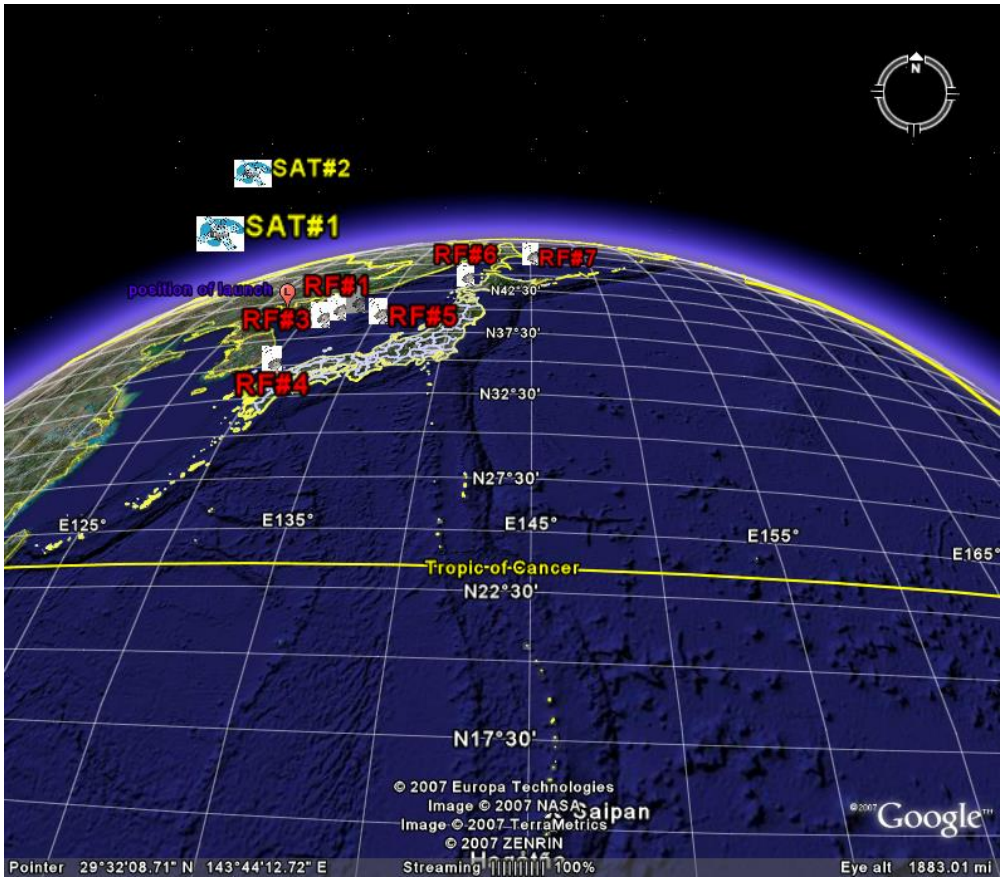

Figure 19. Geographical area of the scenario from a different angle of view (From: 2007 Google/2007 NASA/2007 Europa Technologies Image)

Figure 20 depicts the trajectory of the missile as generated by the IMPULSE program. The type of the missile is a "Sample Unclassified Model." The flight of the missile takes about 26 minutes to cover the distance from Asia to the North American continent. Of the two red lines in Figure 20, one represents the actual trajectory in the air and the second is the footprint on the earth. This graph covers the first 402 sec of the flight. The separation of the booster takes place approximately 65 sec after the launch (when the blue line becomes red) and its trajectory after the separation is the red line. The missile launch position is N40^{o} 51' 17'' and E 129 ^{o} 39'58'' moving toward the East [2].

Figure 20. Trajectory of the Ballistic missile

The parameters of the launched missile selected in the IMPULSE program are given in Table 5 [2].

Parameters	Inputs
Type	'SampleUnclassModels'
Missile	"(U) BOOST Unclassified Sample"
Latitude	N40^{o} 51' 17''
Longitude	E 129^{o} 39'58''
Altitude	20 m
Azimuth	33^{o}
Kick angle	11.5^{o}

Table 5. Ballistic Missile parameters. IMPULSE program inputs.

Figure 21 depicts a panoramic view of the earth and the trajectory of the missile as well as its footprint on the ground for an interval of 1239 sec.

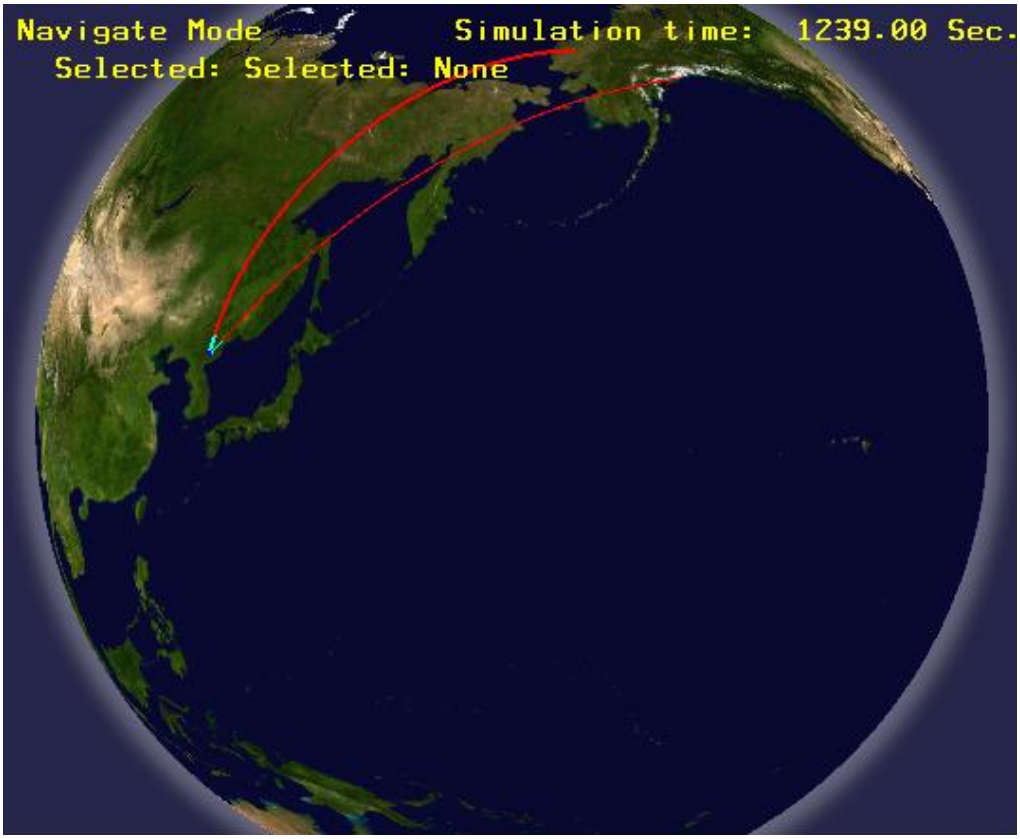

Figure 21. Panoramic view of the ballistic missile's trajectory.

A. RADAR PERFORMANCE

In this section, the results of individual radars as well as the results of data fusion based on the track score mechanism developed in Chapter III are reported.

Figure 22 shows the trajectory of the missile as tracked by RF #1. The red spot on this 3D graph is the position of the radar relative to the missile launch site. The red line on the trajectory is the output of the IMPULSE program. The blue line represents the tracking of the radar. The radar follows the trajectory of the missile closely. At 65 sec, the separation of the booster takes place, which is depicted on the graph by the small curved line.

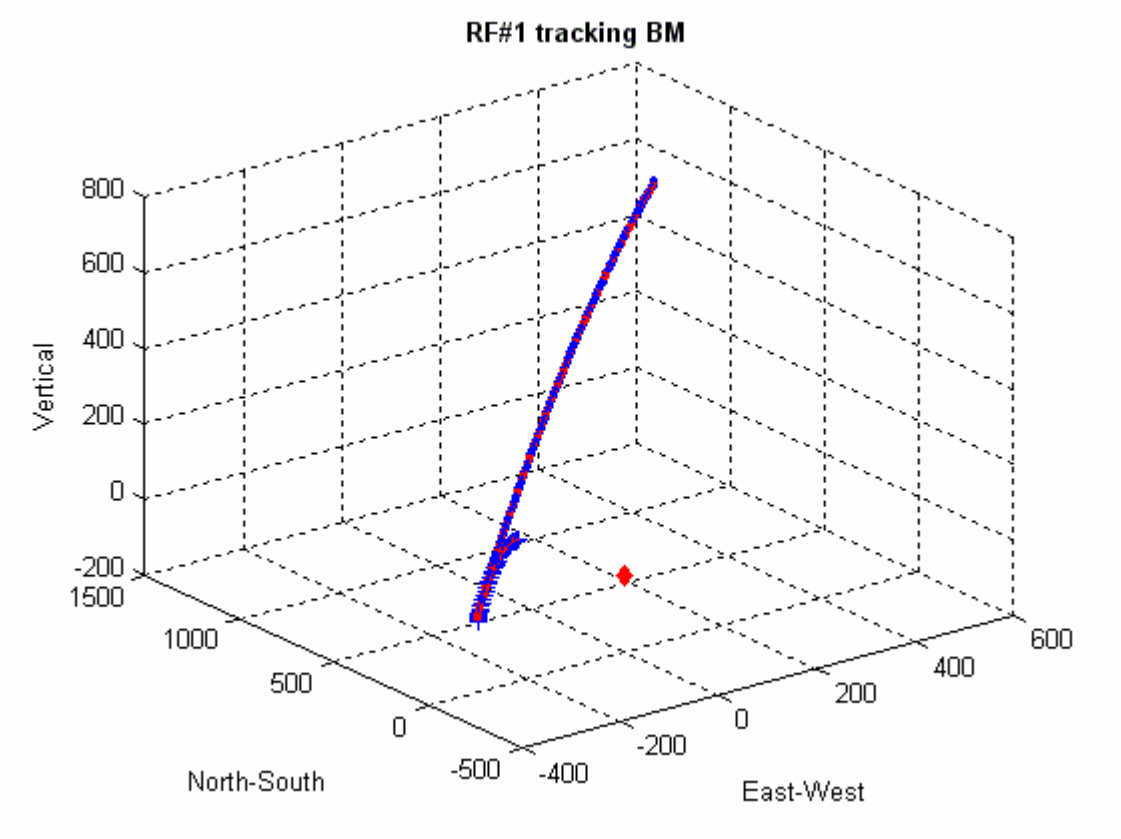

Figure 22. Ballistic missile trajectory from radars #1.

The trajectories from the other six radars deployed in this simulation are depicted in Figures 23 and 24.

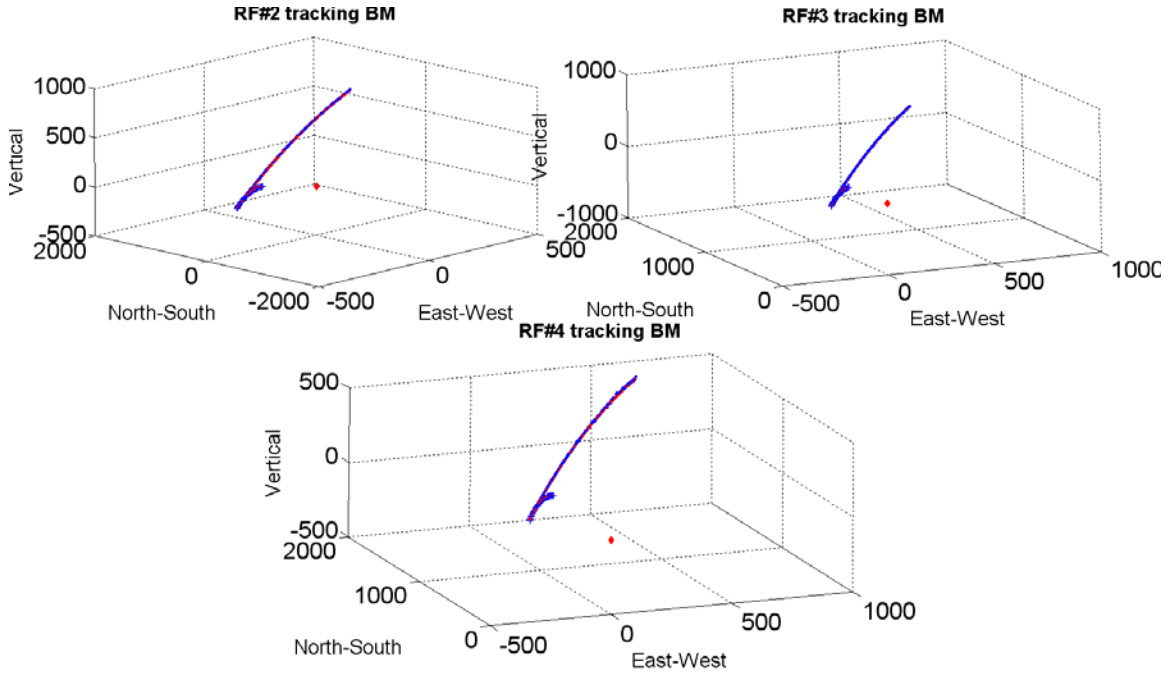

Figure 23. Ballistic missile trajectories from Radars #2, #3, and #4

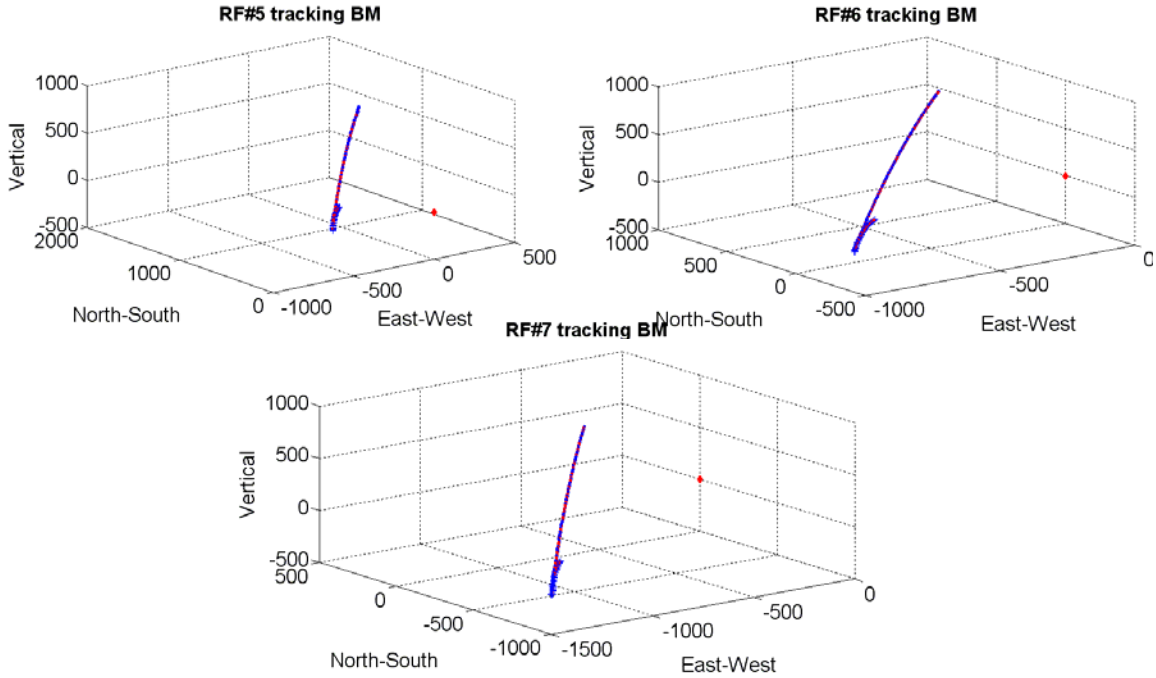

Figure 24. Ballistic missile trajectories from radars #5, #6, and #7.

After the separation of the booster at $t = 65$ sec, the radar follows the missile and the booster. The missile's trajectory (green dashed line) is the upper stage. Booster's trajectory is (red dashed line) is the lower stage. As expected, at the beginning the SNR is large and enough to achieve good tracking, but as the time passes the missile moves away from the radar, so the SNR decreases.

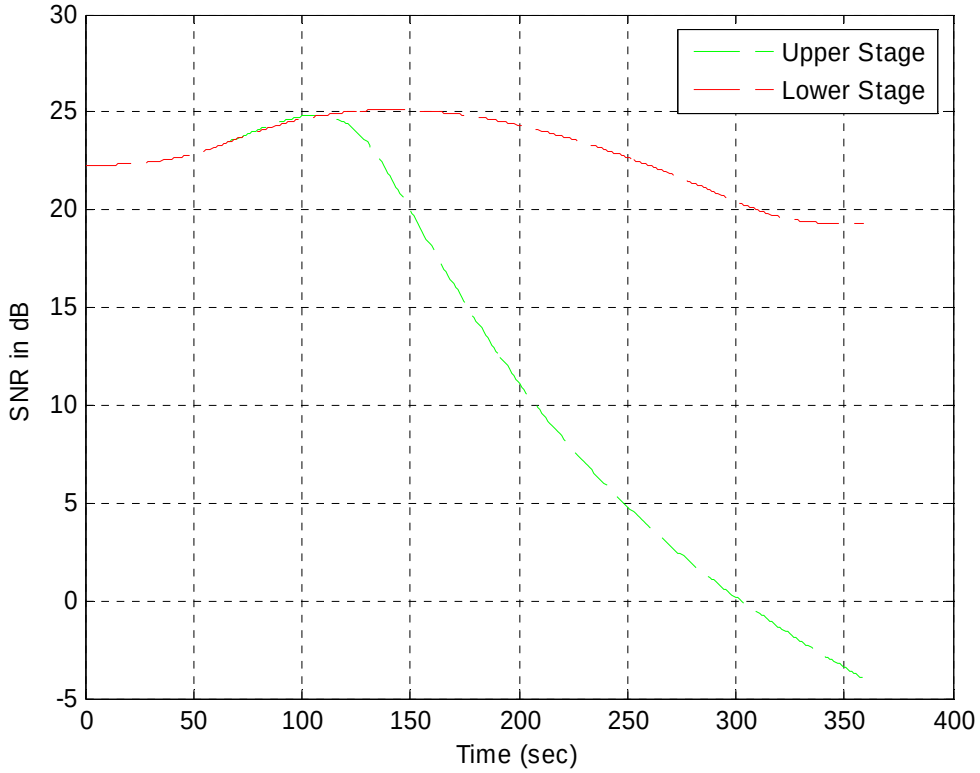

Figure 25. SNR versus Time for the Radar #1

Figures 26 and 27 represent the SNR performance of the other six radars. Taking the position of the sensors relative to the missile into account, the three first sensors (RF#1, RF#2, RF#3) have better performance compared to the fourth sensor (RF#4). The fifth sensor (RF#5) has the same response as the previous sensors but provides smaller values than the first three sensors because it is placed away form the route of the missile. For the next two sensors, which are farther away from the launch site, the SNR responses are presented in Figure 27. For RF#6 and RF#7, the beginning values of the SNR are very small, but as the time passes, the missile approaches the sensors, so the values of the SNR

increase. Especially, for the sixth sensor (RF#6), the SNR reaches the peak value at 240 sec of the flight; then the missile moves away from the sensor, so SNR decreases.

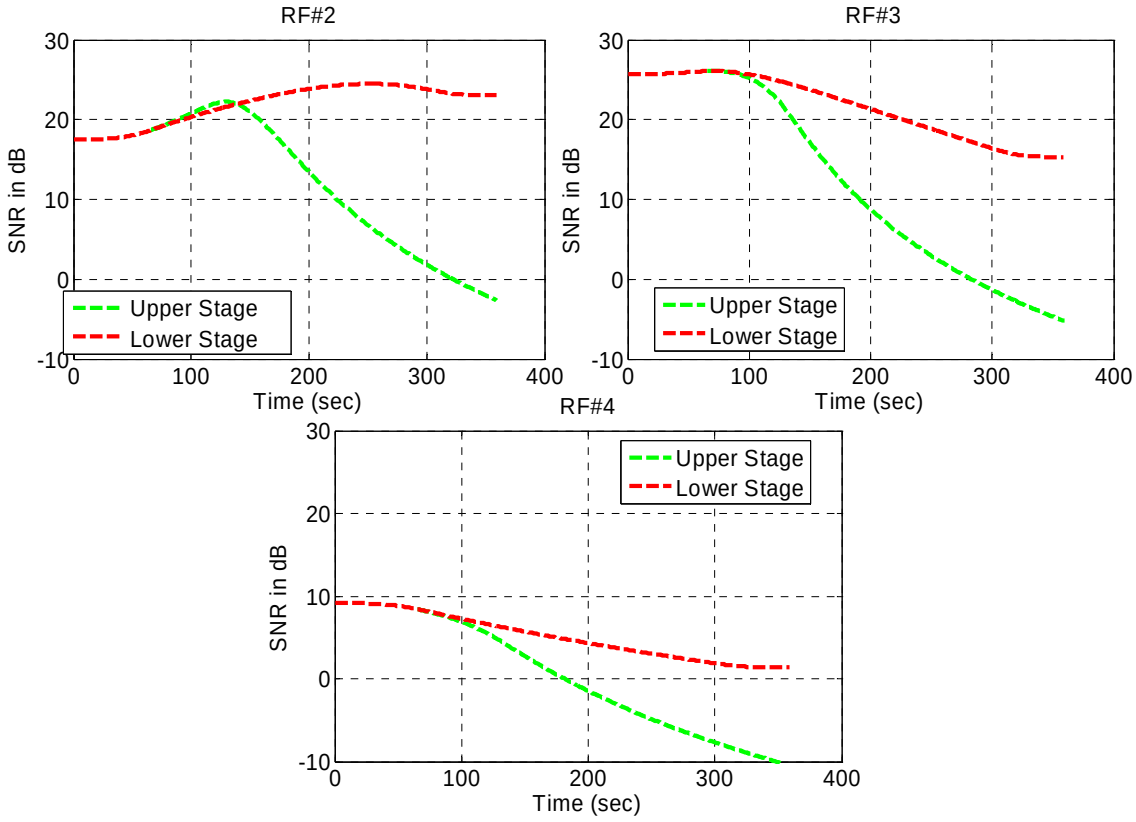

Figure 26. SNR versus Time from Radars #2, #3, and #4.

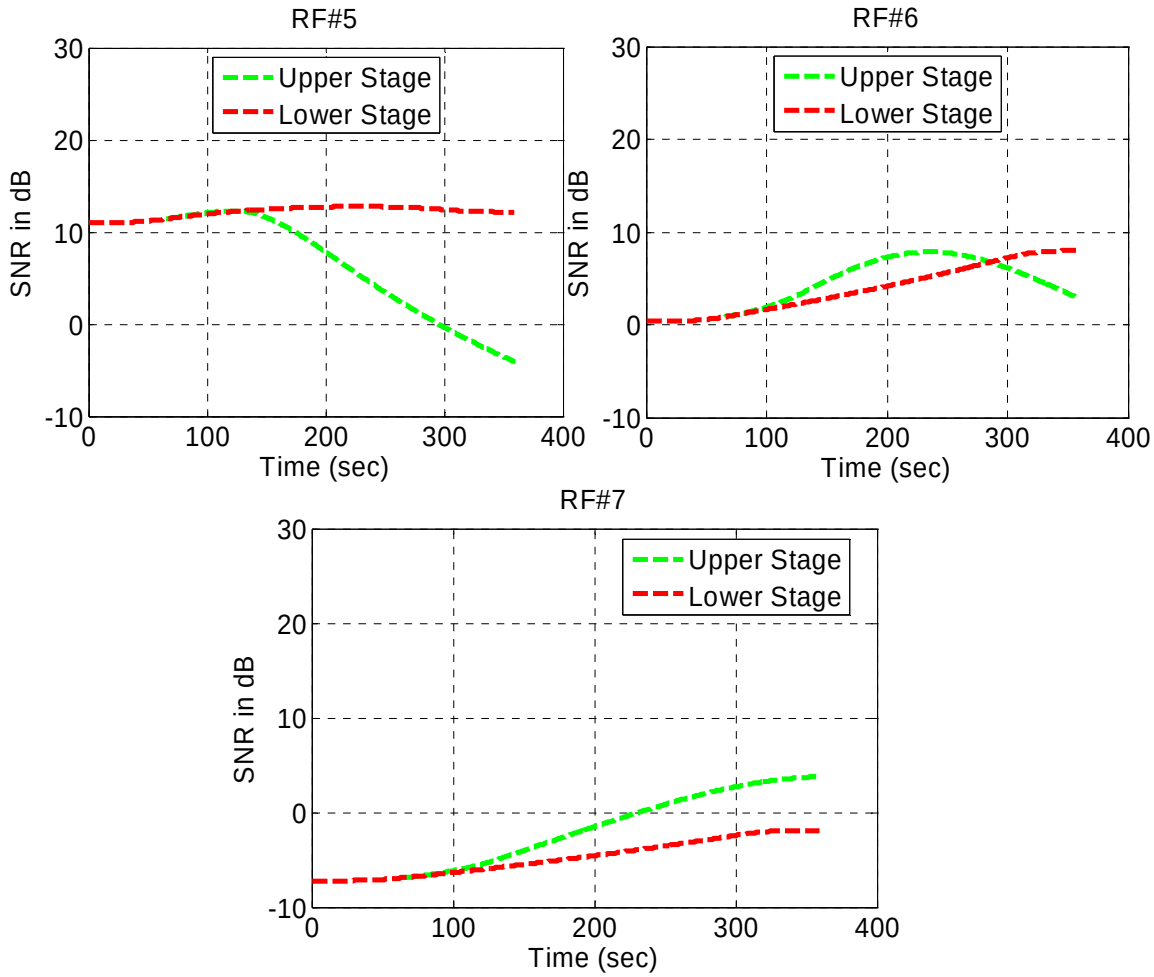

Figure 27. SNR versus Time from Radars #5, #6, and #7.

We now present the data fusion problem. The calculation of the track scoring function is to identify the sensor with the best track file. A track score is calculated for each sensor based on the kinematics of the missile flight parameters and the SNR at the sensor. By using likelihood ratios, the optimum track file of the threat can be determined and the corresponding track file can be transmitted to the Battle Manager Control in order to launch the interceptor vehicle against the threat. Using the optimum track scoring techniques developed in this thesis, the best track file can be sent to the interceptor to guide it to the ballistic threat. This leads to a faster response and the threat can be destroyed inside the territory of the country which launched the missile before the missile employs any countermeasures. Figure 28 shows the track score for three RF sensors as a

function of time (or scans) and demonstrates that during the threat engagement, some sensors have higher track score at certain times while others have a higher track scores at other positions of the threat flight. The objective of the track score processing is to calculate the track score for each track and select the optimum track that should be used to drive the interceptor.

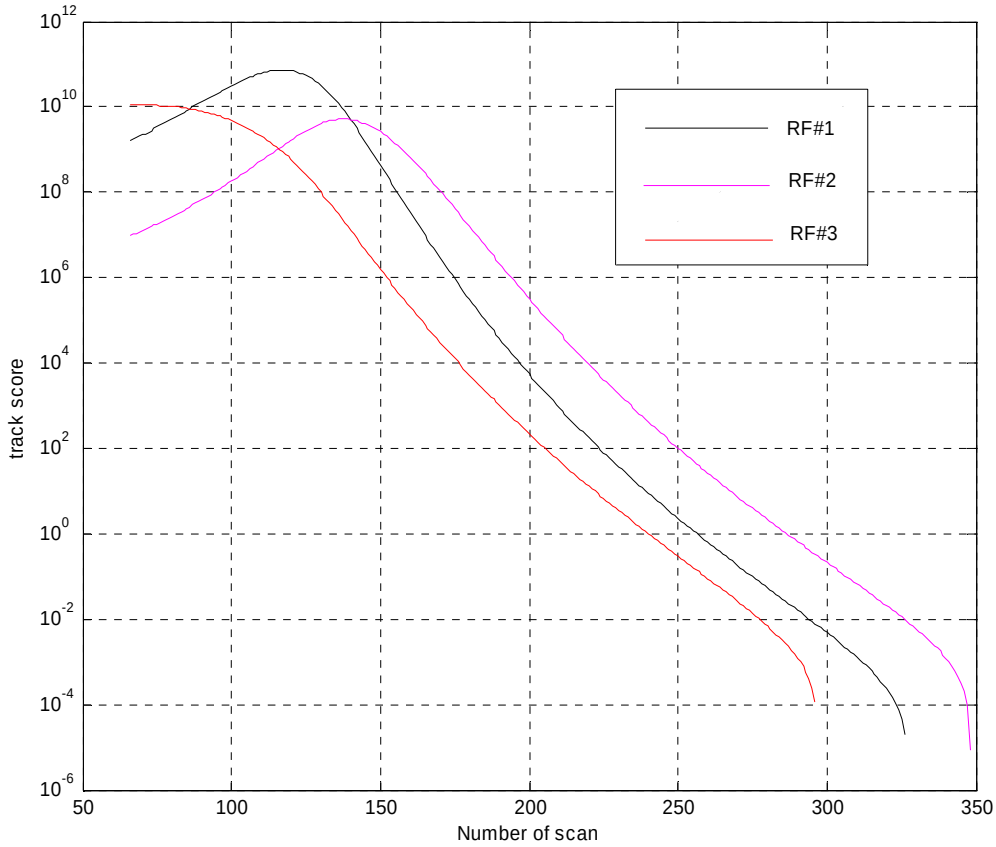

Figure 28. Track scores for Radars #1, #2, and #3.

Based on the track score in Figure 28 at the beginning of the flight, the third radar (RF#3), which is closer to the threat at the beginning, has the best track score quality. As the flight continues, the first radar (RF#1) demonstrates the best track score for the next fifty seconds. Finally, the second radar (RF#2) has the best track score until the end of the boost phase.

B. IR/LIDAR PERFORMANCE

In this section, we present the results of the IR and the LIDAR sensors placed on the satellites platforms, SAT#1 and SAT#2. The IR and LIDAR sensors on each platform have the same design parameters. In Chapter II, the SNR as a function of time for the IR and LIDAR sensors placed on SAT#1 were shown (Figure 9). Figure 29 presents the SNR as a function of time for the IR sensors placed on SAT #1 and SAT#2.

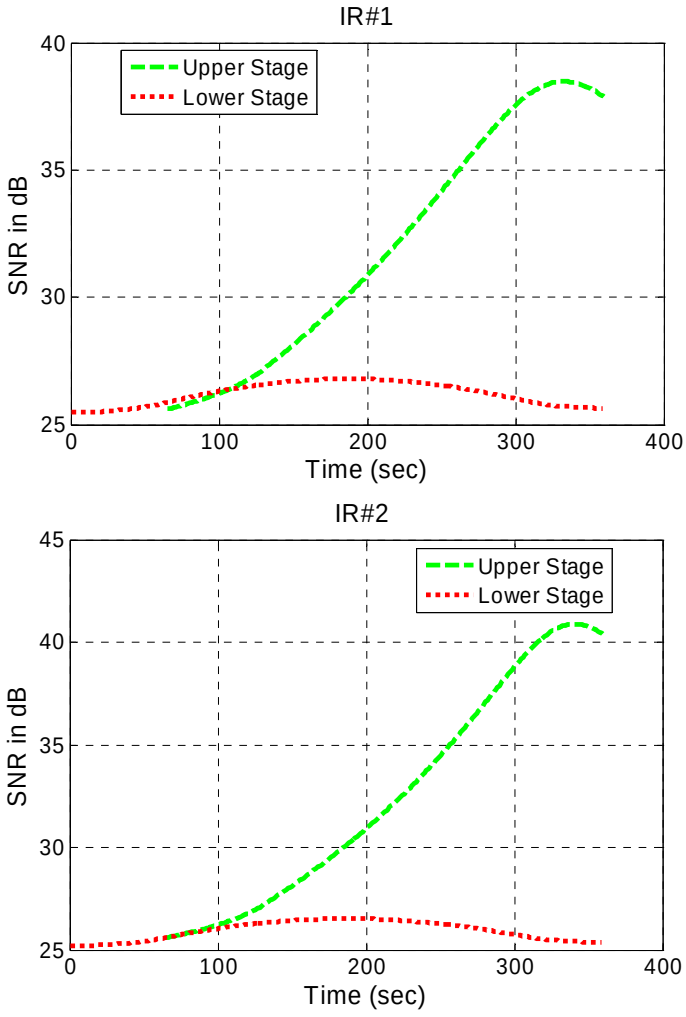

Figure 29. SNR versus time for the IR systems on SAT#1, and SAT#2

Comparing the two plots in Figure 29 for the two IR sensors on SAT#1 and SAT#2, both IR systems show satisfactory performance at the beginning of the flight, having approximately the same value of 25 dB. As the time passes, the SNR for both IR

sensors increases due to the fact the missile approaches the two platforms. The second sensor has better performance as its peak is approximately 42 dB versus 38 dB for the first sensor. Then SNR starts to decrease for both sensors as the missile moves away from the two platforms.

The LIDAR sensors are placed on the same platforms as the IR sensors; the SNR performance of the LIDAR on SAT#1 was shown in Figure 10. Figure 30 presents the SNR of the LIDAR sensors placed on SAT#1 and SAT#2. (The SNR plot of LIDAR #1 is repeated here from Figure 10).

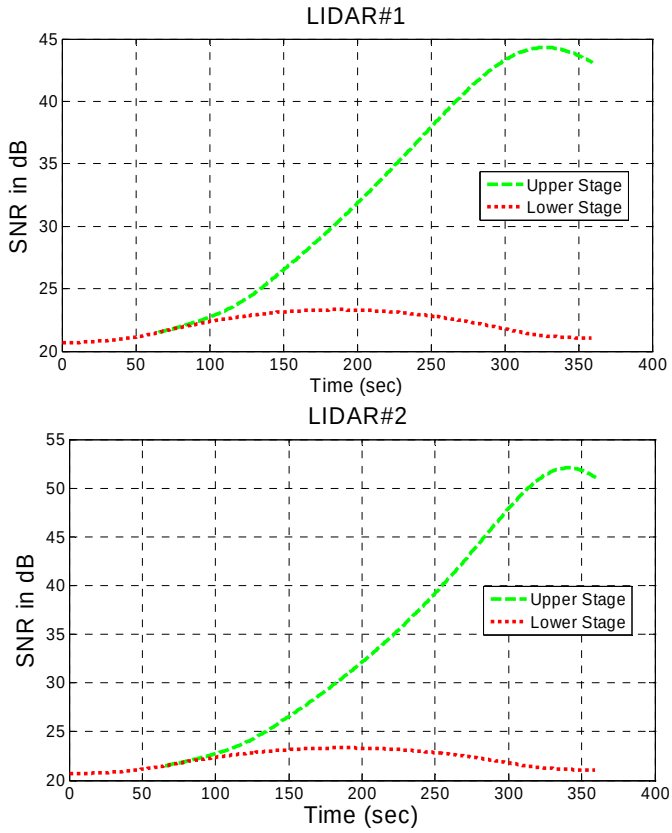

Figure 30. SNR versus time for LIDAR systems on SAT#1, and SAT#2.

Comparing the two plots in Figure 30, the two systems provide the same performance at the beginning of the trajectory as the values of SNR are the same and

approximately equal to 20 dB. As the time passes, the second system performs better than the first system. The peak of the second system is equal to 51 dB compared 44 dB for the second system.

Also, from Figures 29 and 30, the graphs are similar in shape. Only the values of the SNR are different in each graph. Even thought the graphs have been derived from different sensors (IR and LIDAR), their tracking responses are the same. Thus, two different sensors placed on the same platform confirm the trajectory of the missile.

In summary, in this chapter, the results from the simulation for the seven ground radars as well as the results for the spaceborne IR and LIDAR sensors were presented. Also, the results for the data fusion of the radars were presented. Finally, the performance of the spaceborne IR and LIDAR sensors is compared for evaluating the accuracy of the simulation to detect a ballistic missile in the boost-phase.

V. CONCLUSION

In this thesis, a scenario of many different types of sensors in the vicinity of a launched ballistic missile is studied. The main goal was the evaluation of the performance of these sensors during the boost-phase stage of the missile's flight. The SNR of the sensors is used as a figure of merit.

Seven X-band, ground based radars with the same parameters are deployed at different positions. Observing the results of the radars, it is inferred that the distance between the radar and the target is the basic factor to be taken into account for evaluating the performance of the sensor in the data fusion process.

Two IR sensors are deployed in two LEO satellites in order to evaluate their performance during boost-phase. They have an advantage over radars due to their capability to detect the radiation of the missile in this phase. Two LIDAR sensors are also deployed on the same platforms along with the IR sensors. The LIDAR sensor is used to provide the third dimension, the range, which an IR sensor cannot calculate. Based on the results, it is inferred that the use of the LEO satellite supported by IR sensors improves the detection and tracking performance of a ballistic target in the first stage of its flight. The drawback is that the area covered by a LEO satellite for surveillance is limited, so a network of LEO satellites is required for covering the Earth.

The next goal of the thesis was the fusion of the radar sensor data. The technique of likelihood ratios for tracking of each sensor is used. The evaluation provides results about the performance of each sensor with respect to the scan number, which in this work represents the time of the flight.

A. SUGGESTIONS FOR FUTURE WORK

The implementation of different types of radar in the vicinity of the missile launch site can be an issue for further investigation. Radars with different parameters, such as transmitted power, frequency, PRF, antenna gain and antenna temperature based on

actual sky temperatures for the radar frequency and beam elevation angles of interest will present a more realistic scenario for the data fusion problem. In this situation, the distance between the sensor and the target is not the primary factor for evaluating the data fusion problem.

The data fusion problem for the IR sensors based on the likelihood ratio can be studied in a future research. The fusion of the IR sensor data in boost phase is not the primary goal as the function of IR is only to detect the ballistic missile. In the next stages is where the IR sensor can contribute to the tracking of the missile hence the data fusion problem.

A study involving deployment of multiple simultaneously launched ballistic missiles is of interest. A network of LEO satellites with IR sensors may be employed to discriminate targets and determine the tracks of multiple targets.

APPENDIX. FLOW CHART CODE

The MATLAB code used in this work is based on the code of Reference [2]. The code has been modified in order to include the function of the data fusion among the radars and the deployment of the IR and LIDAR sensors. Figures 31, 32 and 33 present the flow charts for data fusion.

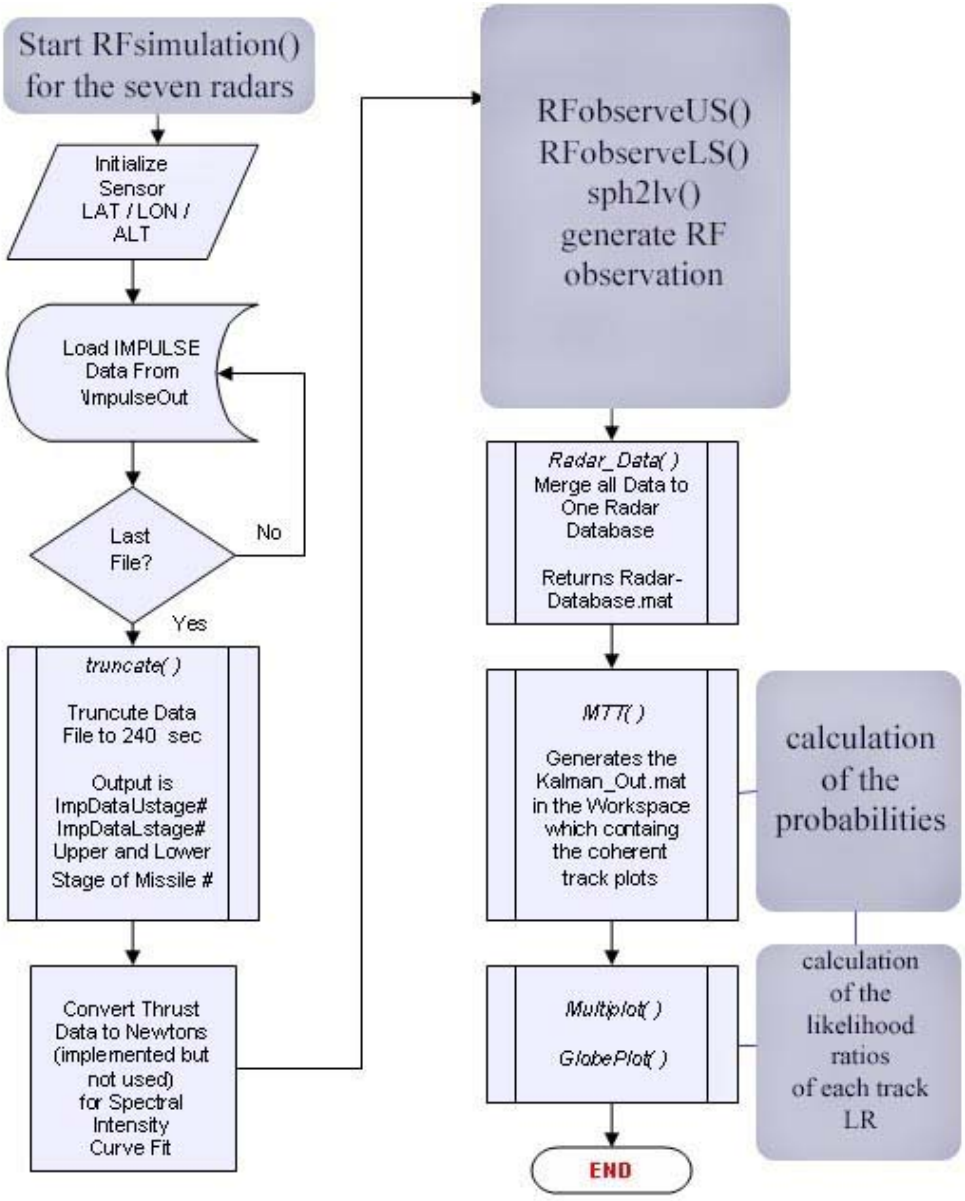

Figure 31. RFsimulation() for the seven radars

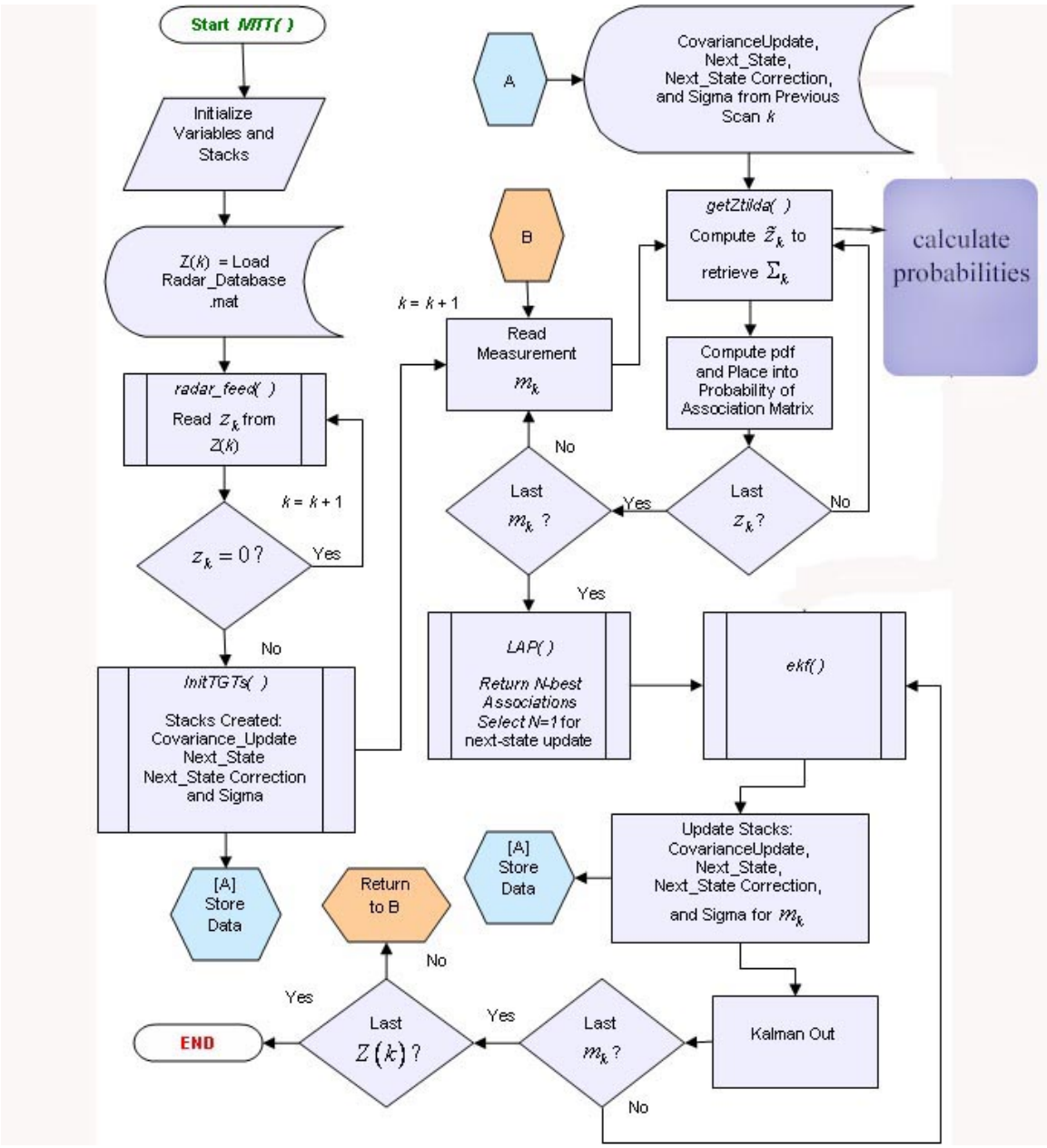

Figure 32. MTT() including the data fusion problem

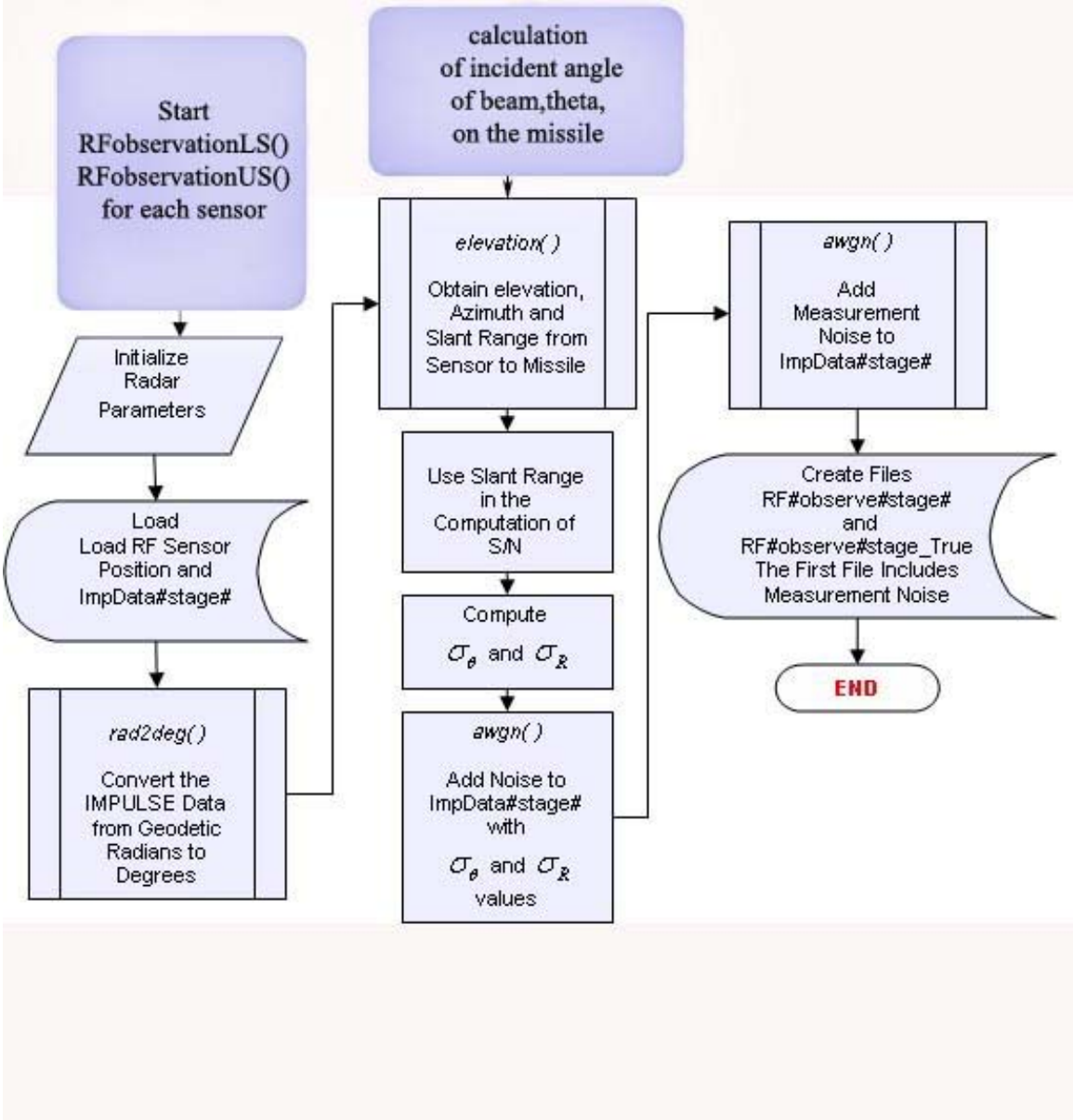

Figure 33. RFobservation() for all the sensors

Figures 34 and 35 present the flow chart for the LIDAR sensors

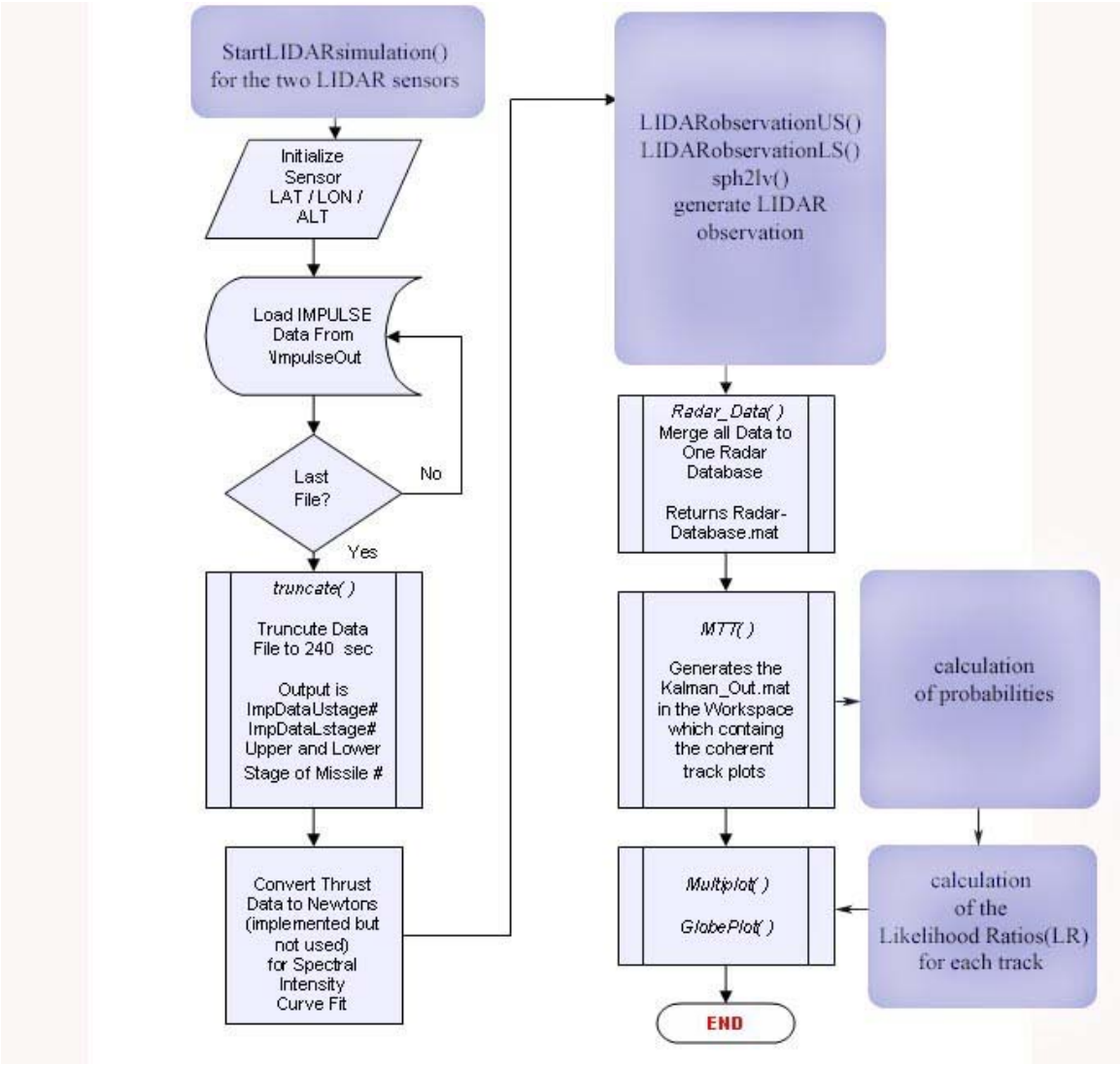

Figure 34. LIDARsimulation() for the two LIDAR sensors

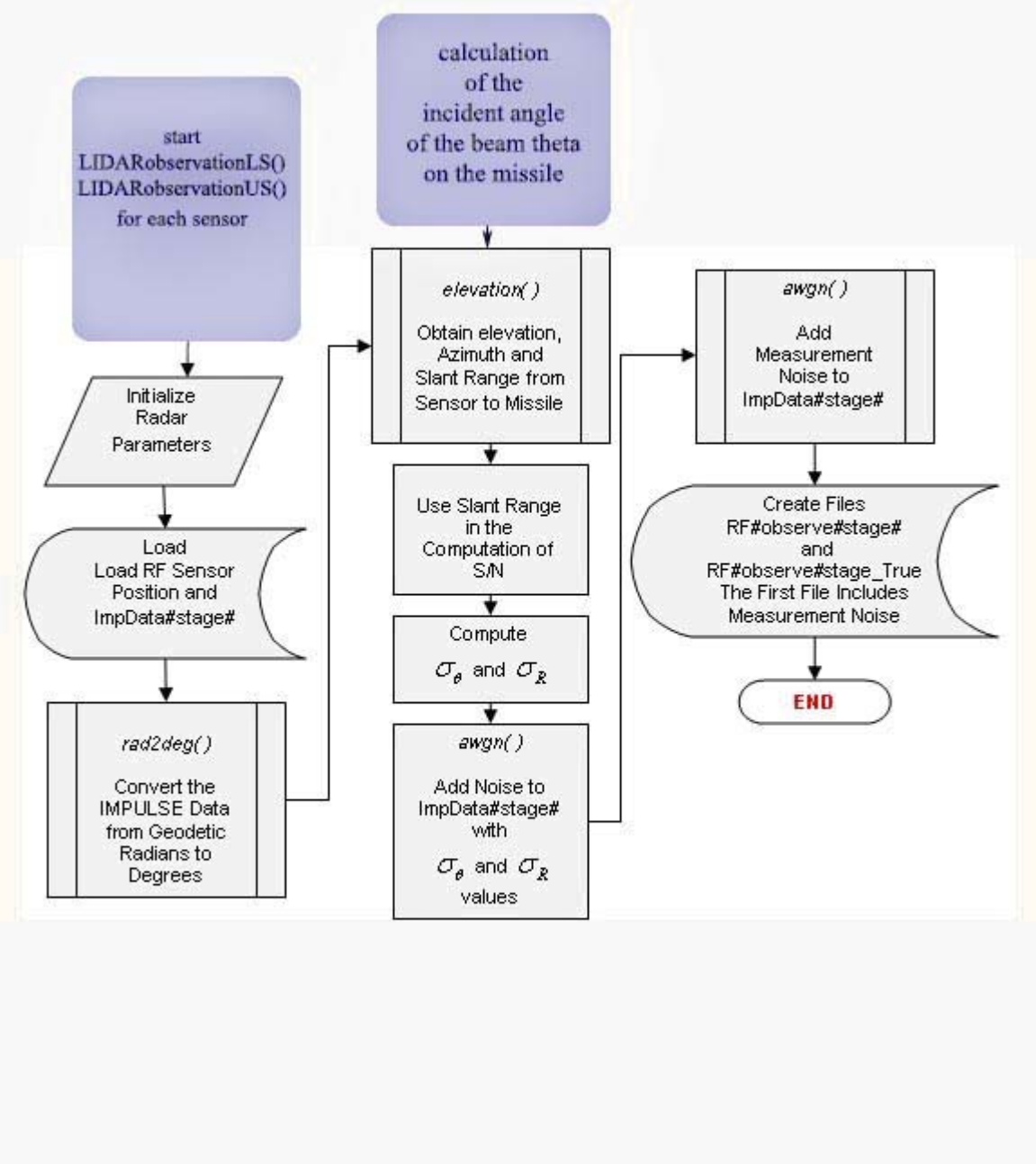

Figure 35. LIDARobservation() for the two LIDAR sensors

Figure 36 presents the flow chart for IR sensors.

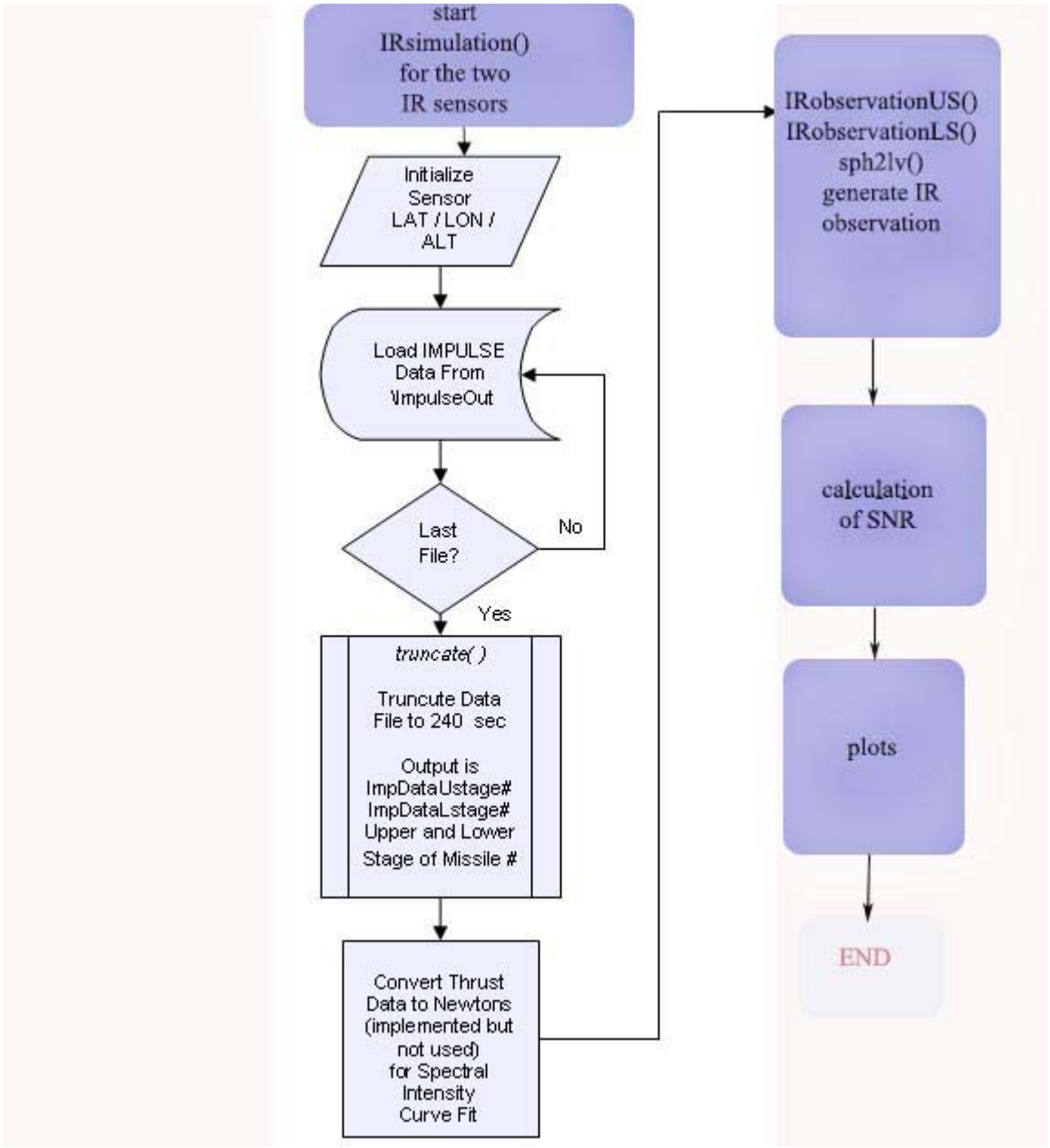

Figure 36. Flow chart for IR sensors

LIST OF REFERENCES

[1] H. Kissinger, "The Threat," March 9, 1995 from http://www.missilethreat.com/ (last accessed June 8, 2007).

[2] B. Radkham. "Efficient Multiple Hypothesis Track Processing of Boost-Phase Ballistic Missiles using IMPULSE-Generated Threat Models," MSEE Thesis, Naval Postgraduate School, Monterey, CA, September 2006.

[3] R. Danchick and G. E. Newman, "A Fast Method for Finding the Exact N-best Hypotheses for Multitargets Tracking," *IEEE Transactions on Aerospace and Electronic Systems* , pp. 550-560, Vol. 29, No 2, 1993.

[4] S. Blackman and R. Popoli, *Modern Tracking Systems*, Norward, NY: Artech House 1999 Publishers, Chapter 2.

[5] G. Waldman and J. Wooton, *Electro-Optical System Performance Modeling*, Norwood, MA: Artech House, 1993

[6] E. L. Dereniak and G. D. Boreman, *Infrared Detectors and Systems*, John Wiley & Sons Inc, 1996.

[7] R. C. Olsen, *Remote Sensing from Air and Space*, SPIE press book, January 2007, Chapter 5.

[8] D. H. Pollock, *The Infrared & Electro-Optic Systems Handbook*, Vol. 7, p.117, SPIE Optical Engineering Press, Bellingham, WA, 1996.

[9] M. Tidrow and W. R Dyer, "Infrared Sensors For Ballistic Missile Defense," *Infrared Physics & Technology*, June. 2001, Vol. 42, no. 3-5, pp. 333-336.

[10] S. Khalil and S. A. Hovanessian, *Introduction to EO Imaging and Tracking Systems*, Norward, NY: Artech House,1993, Chapter 7.

[11] F. Neri, *Introduction to Electronic Defense Systems*, Norward, NY:Artech House, 2n Edition, 2001, Chapter 2.

[12] E. Garrido, "Graphical user interface for a physical optics radar cross section prediction code," Master's Thesis, Naval Postgraduate School, Monterey, CA, 2000.

[13] D. L. Hall, and J. Linas, *Handbook of Multisensor Data Fusion,* CRC Press LLC, May 2001.

[14] Y. Bar-Shalom, X. Li. Rong and T. Kirubarajan, *Estimation with applications to Tracking and Navigation,* John Wiley & Sons Inc, 2001, p. 73.

[15] P. F. Singer and D. M. Sasaki, “The Heavy Tailed Distribution of a Common CFAR Detector,” *Signal and Data Processing of Small Targets 1995*, Proc. SPIE 2561, 1995, pp.124–140.

INITIAL DISTRIBUTION LIST

1. Defense Technical Information Center
   Ft. Belvoir, Virginia

2. Dudley Knox Library
   Naval Postgraduate School
   Monterey, California

3. Jeffrey B. Knorr
   Department of Electrical and Computer Engineering
   Monterey, California

4. James H. Luscombe
   Department of Applied Physics
   Monterey, California

5. Phillip E.Pace
   Department of Electrical and Computer Engineering
   Monterey, California

6. Murali Tummala
   Department of Electrical and Computer Engineering
   Monterey, California

7. Gamani Karunasiri
   Department of Applied Physics
   Monterey, California

8. Michael James
   Department of Electrical and Computer Engineering
   Monterey, California

9. Dimitrios Patsikas
   Hellenic Navy
   Athens,Greece

10. GEN/B2
    Hellenic Navy
    Athens,Greece

11. Ms. Deborah Stiltner
    Missile Defense National Team
    Crystal City, Virginia